International Journal for Parasitology: Drugs and Drug Resistance 16 (2021) 174–187

Contents lists available at ScienceDirect

International Journal for Parasitology: Drugs and Drug Resistance

journal homepage: www.elsevier.com/locate/ijpddr

Comparison of electrophysiological and motility assays to study anthelmintic effects in *Caenorhabditis elegans*

Steffen R. Hahnel [a,1,*], William M. Roberts [b], Iring Heisler [a], Daniel Kulke [a,2], Janis C. Weeks [b]

[a] Elanco Animal Health, Monheim, Germany
[b] InVivo Biosystems Inc. (formerly NemaMetrix Inc.), Eugene, OR, USA

ARTICLE INFO

Keywords:
Caenorhabditis *elegans*
Nematode pharynx
Electropharyngeogram (EPG)
8-channel chip
ScreenChip
wMicroTracker
Macrocyclic lactones
Levamisole
Pharyngeal pumping
Anthelmintics

ABSTRACT

Currently, only a few chemical drug classes are available to control the global burden of nematode infections in humans and animals. Most of these drugs exert their anthelmintic activity by interacting with proteins such as ion channels, and the nematode neuromuscular system remains a promising target for novel intervention strategies. Many commonly-used phenotypic readouts such as motility provide only indirect insight into neuromuscular function and the site(s) of action of chemical compounds. Electrophysiological recordings provide more specific information but are typically technically challenging and lack high throughput for drug discovery. Because drug discovery relies strongly on the evaluation and ranking of drug candidates, including closely related chemical derivatives, precise assays and assay combinations are needed for capturing and distinguishing subtle drug effects.

Past studies show that nematode motility and pharyngeal pumping (feeding) are inhibited by most anthelmintic drugs. Here we compare two microfluidic devices ("chips") that record electrophysiological signals from the nematode pharynx (electropharyngeograms; EPGs) — the ScreenChip™ and the 8-channel EPG platform — to evaluate their respective utility for anthelmintic research. We additionally compared EPG data with whole-worm motility measurements obtained with the wMicroTracker instrument. As references, we used three macrocyclic lactones (ivermectin, moxidectin, and milbemycin oxime), and levamisole, which act on different ion channels. Drug potencies (IC_{50} and IC_{95} values) from concentration-response curves, and the time-course of drug effects, were compared across platforms and across drugs. Drug effects on pump timing and EPG waveforms were also investigated. These experiments confirmed drug-class specific effects of the tested anthelmintics and illustrated the relative strengths and limitations of the different assays for anthelmintic research.

1. Introduction

As important parasites of humans, animals and plants, nematodes have a tremendous impact on global health and socioeconomic development (Lustigman et al., 2012; Hotez et al., 2014), but their control relies on only a limited repertoire of chemical drug classes that exhibit anthelmintic activity (Kotze et al., 2014). Moreover, extensive administration of these anthelmintic drug classes has led to geographically widespread resistance in veterinary medicine (Kotze et al., 2014) and an increasing threat of resistance in human parasites (Schwab et al., 2005; Diawara et al., 2013; Krücken et al., 2017). To face this alarming trend, a detailed understanding of both mechanisms of anthelmintic action as well as of resistance development is urgently needed to improve existing treatment strategies and to support the discovery of novel drug classes.

Most anthelmintic drug classes affect the neuromuscular system of nematodes by interacting with ion channels and receptors on neurons and muscles (Wolstenholme, 2011; Holden-Dye and Walker, 2014). Depending on the tissue- and stage-specific expression of their main molecular targets, anthelmintic drugs induce distinct class-specific phenotypes. For example, the broadly used anthelmintic drug class of macrocyclic lactones (MLs) acts on an invertebrate-specific family of ion channels, the glutamate-gated chloride channels (GluCls), which are

* Corresponding author.
E-mail addresses: Steffen.r.hahnel@gmail.com (S.R. Hahnel), bill.roberts@invivobiosystems.com (W.M. Roberts), iring.heisler@elancoah.com (I. Heisler), daniel.kulke@elancoah.com (D. Kulke), janis.weeks@invivobiosystems.com (J.C. Weeks).
[1] Current address: Rupt Sur Moselle Str. 12, Stadecken-Elsheim, Germany.
[2] Current address: Iowa State University, Department of Biomedical Sciences, Ames, Iowa, United States. dkulke@iastate.edu.

https://doi.org/10.1016/j.ijpddr.2021.05.005
Received 9 March 2021; Received in revised form 15 May 2021; Accepted 20 May 2021
Available online 2 July 2021
2211-3207/© 2021 The Author(s). Published by Elsevier Ltd on behalf of Australian Society for Parasitology. This is an open access article under the CC BY-NC-ND license (http://creativecommons.org/licenses/by-nc-nd/4.0/).

widely expressed in the neuromuscular system of nematodes (Cully et al., 1994; Dent et al., 2000; Wolstenholme and Rogers, 2005). In several nematode species, including *Caenorhabditis elegans* and gastrointestinal nematodes such as *Haemonchus contortus* and *Ascaris suum*, MLs induce paralysis (Kass et al., 1980; Gill et al., 1991; Dent et al., 2000) of the body wall and pharyngeal muscles, thereby inhibiting motility and food uptake (; Geary et al., 1993; Brownlee et al., 1997; Ardelli et al., 2009). Other drugs, such as levamisole (LEV), exert their anthelmintic activity by modulating specific nicotinic acetylcholine receptors (nAChRs) (Holden-Dye and Walker, 2014), which are pentameric ion channels located in the postsynaptic membrane at cholinergic synapses. In nematodes, nAChRs are typically heteromultimers of five subunits, whose composition can influence drug specificity (Martin et al., 2012; Kotze et al., 2014; Blanchard et al., 2018). Although nAChR subunits are expressed throughout the nervous system, those that form the *C. elegans* LEV-sensitive nAChRs are located mainly at neuromuscular junctions on body wall muscles. LEV-induced opening of these excitatory ion channels causes a hypercontraction phenotype (Martin et al., 2005). In addition to these class-specific characteristics, different chemical derivatives within a single anthelmintic drug class show different physicochemical properties that potentially influence potency (e.g., target affinity) as well as pharmacokinetics (e.g., solubility, permeability, metabolism, distribution) in nematodes (Ardelli et al., 2009; Demeler et al., 2014; Stasiuk et al., 2019). Thus, unraveling intra- and inter-class specific phenotypes can potentially inform mode of action studies and support anthelmintic drug discovery, with the need for precise assays and assay combinations that can capture and distinguish subtle drug effects.

Most *in vitro* assays for evaluating anthelmintic drug activity rely on robust phenotypic read-outs that can be optimized for high throughput, such as nematode development, motility, reproduction, and survival (Lai et al., 2014; Burns et al., 2015; Partridge et al., 2018; Spensley et al., 2018; Zamanian et al., 2018). These read-outs typically do not, on their own, reveal where a test compound acts (e.g., the tissue or molecular target). In contrast, electrophysiological assays allow more direct investigation of drug effects on the neuromuscular system of nematodes. Intracellular electrical recording techniques, including two-electrode voltage clamp and patch-clamp, have been applied to *A. suum, Brugia malayi* and *Dirofilaria immitis* muscles (Colquhoun et al., 1991; Martin and Robertson, 2000; Kashyap et al., 2019; Verma et al., 2020). In *C. elegans,* both patch-clamp and extracellular electrical recording methods have been used to study neuromuscular junctions on body wall and the pharynx (Cook et al., 2006; Richmond, 2006). Although these approaches can provide fundamental insights into the mode of action of major anthelmintic drug classes (Martin and Robertson, 2000; Holden-Dye and Walker, 2006), they are technically challenging and labor-intensive and therefore not commonly included in drug discovery pipelines.

With recent innovations in microfluidic chip technology for *C. elegans* research (San-Miguel and Lu, 2013; Muthaiyan Shanmugam and Subhra Santra, 2016), novel approaches became available to make electrophysiological recordings in a more user-friendly manner that allows increased throughput compared to classical electrical recording techniques (Lockery et al., 2012; Hu et al., 2013). Lockery et al. (2012) developed a microfluidic chip that records electropharyngeograms (EPGs) — the electrical signals emitted by muscles and neurons of the pharynx during pumping — from eight worms simultaneously while perfusing test substances ("8-channel platform"). This technology was subsequently commercialized as a single-channel EPG recording device, the ScreenChip™ (InVivo Biosystems). Microfluidic EPG recordings have been successfully used in *C. elegans* to characterize anthelmintic effects in drug-susceptible and -resistant worm strains (Lockery et al., 2012; Weeks et al., 2018b), as part of a screen for drug library repurposing (Weeks et al., 2018a) and for other applications including *C. elegans* models of human diseases (Huang et al., 2019; Zhu et al., 2020). The 8-channel platform has also been validated in parasitic nematodes including *A. suum* and *Ancylostoma* spp. (Weeks et al., 2016). A different EPG chip was developed in the laboratory of Prof. Lindy Holden-Dye for *C. elegans* (Hu et al., 2013; Calahorro et al., 2019) and plant parasitic nematodes (Hu et al., 2014).

The aim of the present study was to compare the ScreenChip and 8-Channel platform, and the wMicroTracker device (InVivo Biosystems), which measures worm motility, to identify respective strengths and limitations of these assays for anthelmintic research. Three different MLs [ivermectin (IVM), moxidectin (MOX), and milbemycin oxime (MIL)], and LEV, were tested as references on adult *C. elegans*. The experiments recapitulated characteristics of the selected reference compounds and illustrated that electrophysiological and motility assays, individually and/or in combination, provide useful insights for anthelminthic and mode of action studies.

2. Materials and methods

2.1. Nematodes

C. elegans Bristol N2 worms from the Caenorhabditis Genetics Center (CGC; Minneapolis, MN) were grown at 20 °C on Nematode Growth Medium (NGM) agar plates seeded with the OP50 strain of *E. coli*, using standard methods. Synchronous cultures were obtained by bleaching adults to obtain cohorts of eggs (Stiernagle, 2006). Day-1 adult hermaphrodites (12–24 h after the adult molt) were used for all experiments.

2.2. Drugs and solutions

Stock solutions of 5-Hydroxytryptamine hydrochloride (5HT, Sigma-Aldrich #H9523; St. Louis, MO USA) were prepared in M9 buffer (Stiernagle, 2006) at 40 mM, stored at −20 °C and diluted to 10 mM in M9 buffer for experiments; 10 mM 5HT in M9 buffer was termed "M9-5HT" solution. Stock solutions (20 mM in 100% DMSO) were prepared of IVM (Sigma-Aldrich #PHR1380), MOX (Sigma-Aldrich #33746) and MIL (Sigma-Aldrich #Y0001893) and stored at −20 °C. For LEV (Sigma-Aldrich #31742), 1 M stocks were prepared in M9 buffer and stored at −20 °C until further use. Working solutions were prepared daily by diluting stocks into M9-5HT, with maximum final DMSO (Sigma-Aldrich #41640; St. Louis, MO USA) concentrations of 0.1%.

2.3. EPG recordings with the ScreenChip system

The ScreenChip™ (InVivo Biosystems, Eugene, OR, USA) is a commercially available microfluidic platform for EPG recordings of the nematode pharynx. Disposable microfluidic cartridges for the ScreenChip system (Fig. 1A), size SC40, were used for all experiments. For each drug concentration, ~50 synchronized Day-1 adult *C. elegans* were transferred from NGM agar plates into a 1.5 ml conical reaction vessel (Eppendorf, Germany) containing 750 µl M9. Worms were allowed to sink to the bottom of the tube and supernatant was replaced by fresh M9. This washing procedure was repeated three times before worms were incubated for 30 min at 20 °C in 1 ml M9-5HT to which a specific drug concentration had been added.

Immediately following incubation, worms were loaded into the SC40 cartridge (Fig. 1Ai) using suction applied to the outlet port to pull worms from the incubation vessel, through polyethylene tubing (InVivo Biosystems, #PET200) attached to the inlet port, and into the collecting chamber inside the chip. Individual worms were then pulled sequentially into position for recording. The whole procedure was tracked under an inverted microscope (CKX53, Olympus, Japan) to ensure that only one worm at a time occupied the channel and was positioned between the recording electrodes. Worms in the correct position were allowed to settle for 30–60 s before EPG recordings were started. EPG recordings were digitized using NemAquire software (InVivo

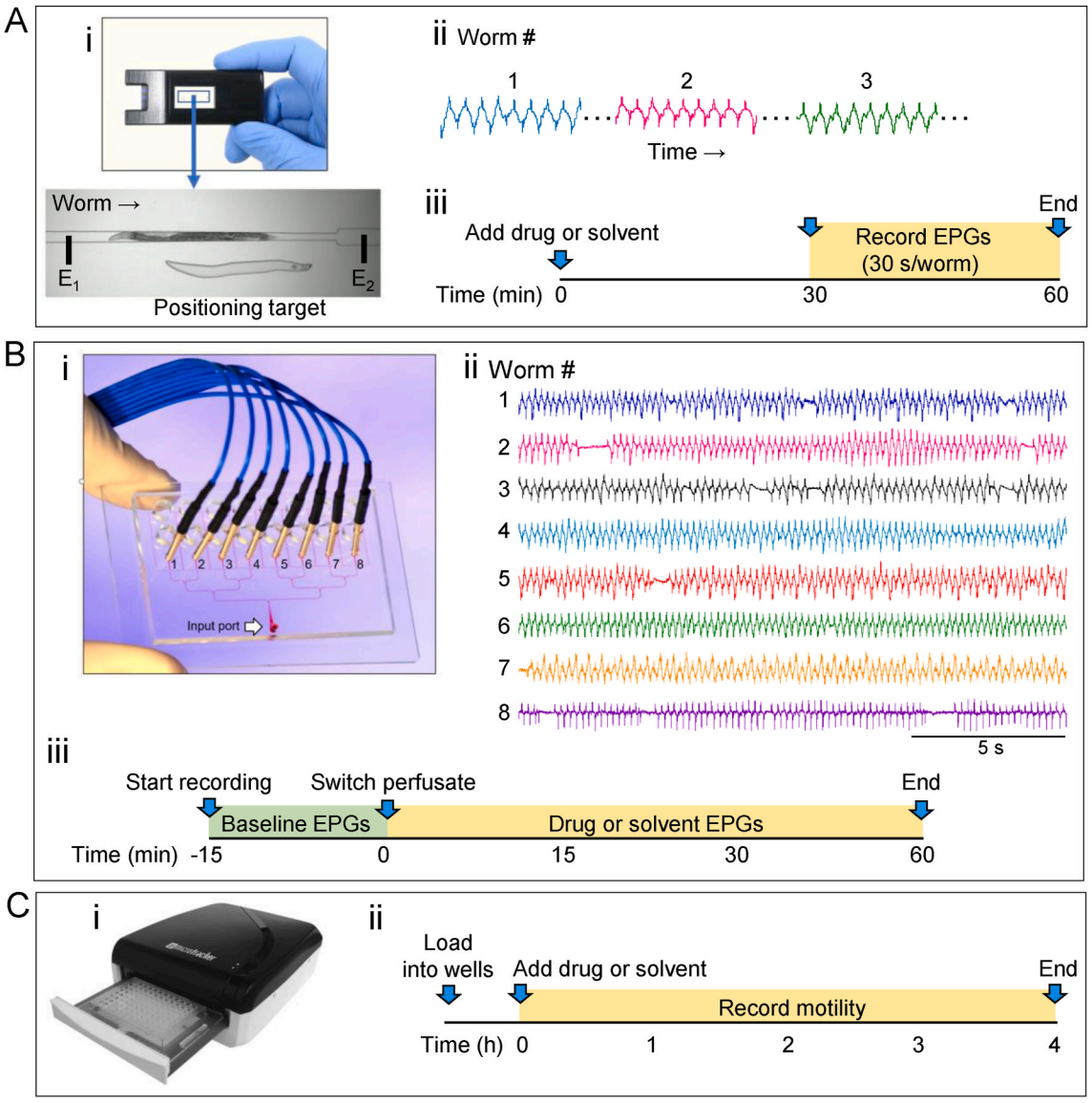

Fig. 1. Experimental setup of microfluidic electropharyngeogram (EPG) recording platforms and wMicroTracker motility assay. A. ScreenChip system. i. The microfluidic chip has an inlet port at one end and an outlet port at the other. Suction applied to the outlet port is used to load worms into a collecting chamber (not shown), where they remain until individual worms are moved into a microchannel (inset) and positioned between two indium tin oxide (ITO) electrodes (represented by E_1, E_2; the electrodes are off screen) for recording. ii. Representation of EPGs recorded serially in the ScreenChip. Gaps (dotted lines) indicate when worms are being positioned between recordings. iii. Experimental protocol. At $t = 0$, drug or solvent was added to worms suspended in M9 buffer containing 10 mM 5HT ("M9-5HT") and incubated for 30 min. Thirty-second recordings from each worm were made between $t = 30$ and $t = 60$ min (orange shading). B. 8-channel EPG platform. i. The chip has a branching network of microchannels (filled with red dye in this image) that distribute worms into 8 recording modules (labelled 1 to 8). Each recording module has an associated recording electrode (blue wire). After loading worms through the input port, the loading tubing is removed and a hollow common reference electrode (not shown) is inserted into the input port, through which solutions are perfused. Reproduced from Lockery et al. (2012) with permission from the Royal Society of Chemistry. ii. The 8-channel chip records EPGs simultaneously from 8 worms, here shown in M9-5HT. iii Experimental protocol. EPGs were recorded for 75 min. During the first 15 min, M9-5HT was perfused to obtain baseline activity (green shading). At $t = 0$ min, the perfusate was switched to M9-5HT containing either drug or solvent control, and recordings were continued for 60 min more (orange shading). C. wMicroTracker. i. The wMicroTracker is a multi-well plate reader that quantifies worm motility in liquid media by counting the number of times an infrared LED microbeam is interrupted by worms moving in a well. ii. Experimental protocol. Worms suspended in M9 containing 0.001% Triton-X were aliquoted into the 96 wells of a plate (~70 worms/well). At time $t = 0$, drug or solvent was pipetted into each well to obtain the desired concentration. Motility was measured continuously for 4 h (orange shading) and analyzed in 30 min bins. (For interpretation of the references to color in this figure legend, the reader is referred to the Web version of this article.)

Biosystems). Each recording lasted 30 s, after which suction was re-applied to pull the worm out of the recording channel and pull a new worm in (Fig. 1Aii-iii). Per experiment, EPGs from 15 worms were recorded for each drug concentration or control condition and cartridges were re-used with successively higher concentrations of the same drug (final ML concentrations: 0.01 μM, 0.03 μM, 0.1 μM, 0.33 μM, 1 μM; final LEV concentrations: 0.1 mM, 0.33 mM, 1 mM, 3.3 mM, 10 mM). Mean pump frequencies were calculated by NemAnalysis software (InVivo Biosystems), which identifies individual pumps by the characteristic E spike and R spike (see Fig. 2A) that mark, respectively, the excitation and relaxation phase of each pump in EPG recordings (Raizen and Avery, 1994). All experiments were repeated in at least three independent replicates.

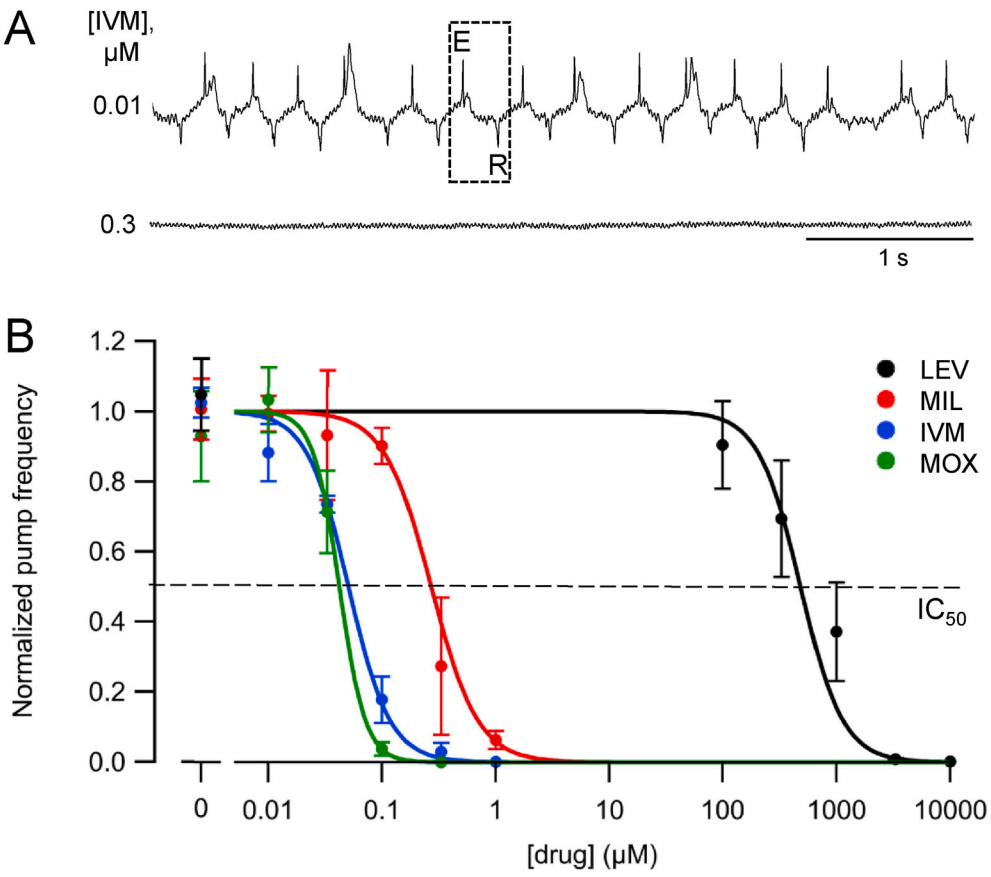

Fig. 2. Effects of MLs and LEV on pump frequency in the ScreenChip. A Representative EPGs recorded from worms in ScreenChips after treatment with two different IVM concentrations for >30 min. Each pump waveform (example marked by dotted box) is demarcated by an E (excitation) spike and R (relaxation) spike (Raizen and Avery, 1994). By convention, the E spike is oriented upward. B. Concentration-dependent inhibition of pharyngeal pumping. Each drug was tested at five concentrations, with mean pump frequencies (Hz) calculated from 15 worms in each of three to four independent experiments per group. The panel shows plots (mean ± S.E.M.) of normalized mean pump frequencies. Hill curves were fit to the normalized data using a maximum likelihood criterion with three free parameters (see Methods). A dashed horizontal line at $y = 0.5$ intercepts the IC_{50} value for each fitted curve; the IC_{50} values appear in Table 1. The three MLs (IVM, MOX, MIL) and LEV all caused a concentration-dependent decrease in pump frequency. MOX and IVM were the most potent, followed by MIL and LEV. Statistical comparisons between IC_{50} values appear in Table 1. Hill slope coefficients: LEV, 2.3; MIL, 2.1; IVM, 2.4; MOX, 3.8.

2.4. Electropharyngeogram (EPG) recordings with the 8-channel platform

Microfluidic chips with 8 EPG recording modules (Fig. 1B) were fabricated using standard soft lithographic methods as described previously (Lockery et al., 2012; Weeks et al., 2018b). Briefly, silicon wafer masters were created using SU-8 2050 resist (Microchem, Newton, MA USA) and replica-molded in polydimethylsiloxane (PDMS; Dow Corning Sylgard 184, Corning, NY USA). PDMS castings were punched to produce ports, inlets and fluid reservoirs, exposed to an oxidizing air plasma and bonded to glass substrates.

Eight-channel EPG recordings were obtained from Day-1 adult *C. elegans* as described in Weeks et al. (2018b). In brief, worms were harvested from NGM agar plates, incubated in M9-5HT for >10 min, pulled up into tubing attached to a syringe and then loaded into the input port of the 8-channel chip by gentle pressure applied to the syringe. The loading operation was observed through a stereomicroscope (AmScope TLB3000, Irvine, CA, USA). The chip design shunts worms away from already-occupied recording modules and thus distributes one worm per module. The head-first vs. tail-first orientation of worms in modules does not affect drug responses at the concentrations tested here (Weeks et al., 2018b). After loading worms, perfusate was pumped continuously into the input port at 6 μl/min (Harvard Apparatus PHD 2000 syringe pump; Holliston, MA USA), with a brief interruption while the perfusion tubing was switched. To minimize the time required to change perfusates, perfusion tubing carrying baseline solution and test solution were switched at the input port. After passing over worms, perfused solutions accumulated in on-chip waste reservoirs that maintained electrical isolation of the 8 recording electrodes. Chips were discarded after one use.

EPG signals (Fig. 1Bii) were amplified and filtered (head-stage conditioning amplifier and A-M Systems model 1700, Carlsborg, WA USA) and sent to a data acquisition system [Micro1401-3, Cambridge Electronic Design (CED), Cambridge, UK] and Spike2 software (version 7.06a, CED) at 2.5 KHz per channel. Spike2 data were down-sampled, exported to Igor Pro (WaveMetrics, Lake Oswego, OR, USA) and analyzed using a custom pump-detection and analysis algorithm (Weeks et al., 2018b). The algorithm optimizes a 6-parameter fitness function to identify the E spikes and R spikes that demark each pump.

The standard experimental protocol (Fig. 1Biii) consisted of a 15 min baseline period in M9-5HT, followed by 60 min perfusion with either test solution (M9-5HT + drug) or solvent control. Final drug concentrations used for ML were 0.1 μM, 0.33 μM, 1 μM, 3.3 μM, 10 μM, and 33 μM (only for MIL). For LEV, final concentrations of 0.1 mM, 0.33 mM, 1 mM, 3.3 mM, and 10 mM were used. EPG recordings were continuous throughout the baseline and test periods. All experiments were performed in three independent replicates.

2.5. Motility assays using the wMicroTracker

The wMicroTracker (InVivo Biosystems; Fig. 1C) is a LED-based assay system that allows drug effects on nematode motility to be recorded over time (Liu et al., 2019; Risi et al., 2019). As with the electrophysiological assays, wMicroTracker experiments were performed using Day-1 adult *C. elegans*. Prior to the experiment, worms were rinsed from NGM agar plates into a 15 ml conical reaction vessel containing M9 + 0.001% Triton-X (Sigma-Aldrich, St. Louis; MO USA). The worms were allowed to sink to the bottom and the supernatant was replaced three times by fresh M9 + 0.001% Triton-X. Approximately 70 worms in 100 μl M9 + 0.001% Triton-X were pipetted into each well of a flat-bottom 96-well microtiter plate (flat bottom, Greiner Bio-One; Germany). All drugs were applied in six different concentrations (including a solvent-only control) with four replicates per plate (final ML concentrations: 0.1 μM, 0.33 μM, 1 μM, 3.3 μM, 10 μM; final LEV concentrations: 3.3 μM, 10 μM, 33 μM, 100 μM, 330 μM). To ensure a final

solvent concentration of 0.1%, drugs were pre-diluted in M9. The experiment was repeated three times independently. All wMicroTracker recordings were 4 h in duration (Fig. 1Cii) and motility values for different experimental groups were analyzed in 30-min time bins.

2.6. Statistical analysis of phenotype assays

Statistical analysis of concentration-response data was performed as in Weeks et al. (2018b) with some modifications. For each phenotypic

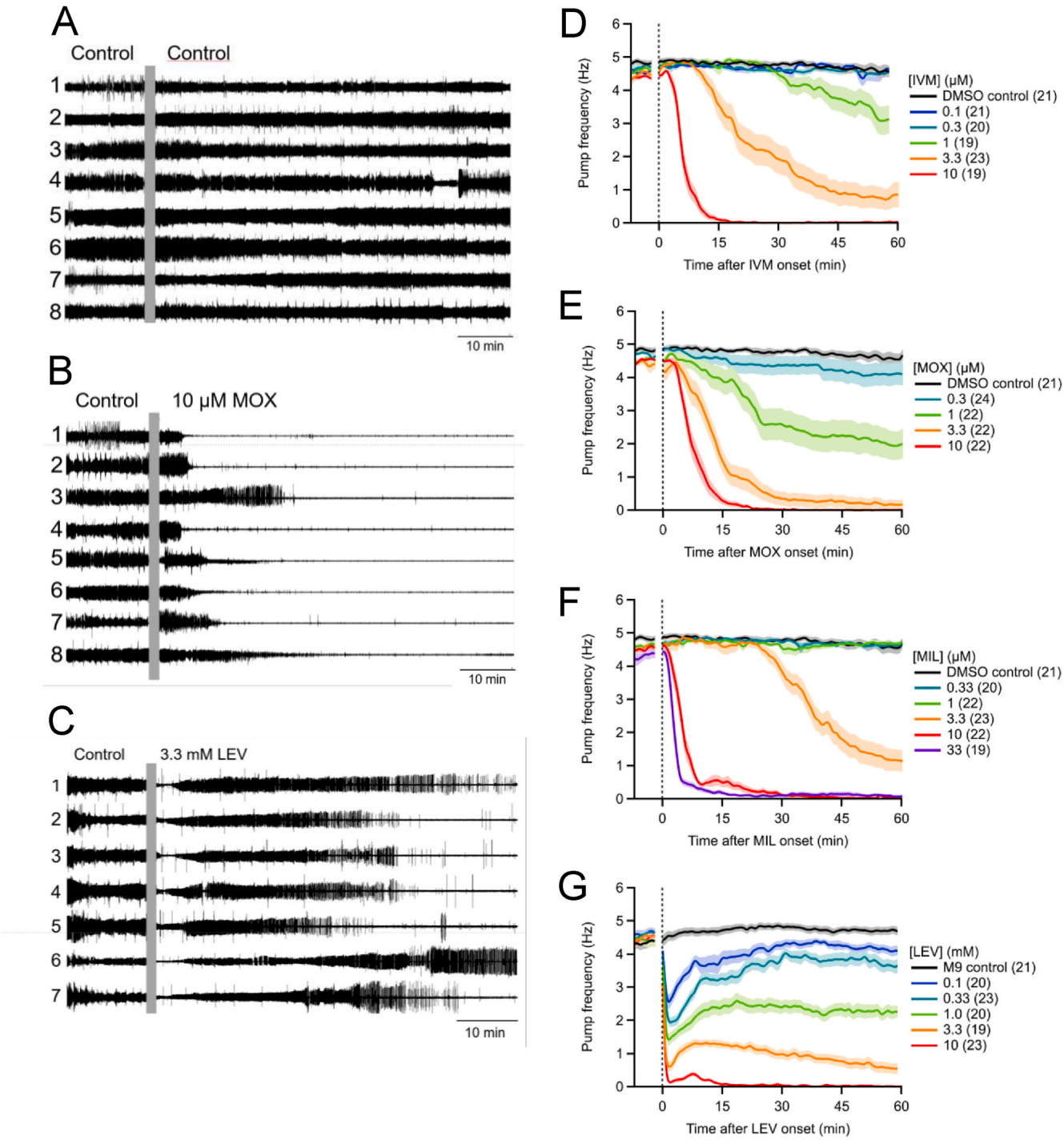

Fig. 3. Time course of ML and LEV effects on pump frequency in the 8-channel platform. A-C each show a set of representative EPG recordings from worms within a single chip. Each worm is numbered. At the compressed time scale shown, changes in amplitude are sometimes apparent, but individual pumps cannot always be resolved. Baseline activity in M9-5HT was recorded for 15 min, followed by switching the perfusate (vertical grey bar) to M9-5HT containing the indicated solution. A. Pumping continued steadily when switched from M9-5HT to M9-5HT. B. In 10 μM MOX, all worms quit pumping by ~25 min. C. In 3.3 mM LEV, pumping frequency transiently decreased, showed partial recovery and then, in most worms shown, decreased again. D-G are plots of pump frequency [mean (line) ± S.E.M. (shading)] over time in different concentrations of the drugs as indicated, with the number of worms in each treatment group in parentheses. In each plot, the final 5 min of baseline pumping is shown and the electrical artifact from switching the perfusate is blanked. A vertical dotted line indicates $t = 0$ when the new solution reached the worms. The DMSO concentration in all groups was 0.1%. The MLs (D–F) all caused a smooth, concentration-dependent decrease in pump frequency over time. In contrast, LEV (G) showed transient and sustained phases of inhibition (Weeks et al., 2018b).

assay we calculated the mean response (m_i) and standard error of the mean (σ_i) at each drug concentration (x_i) by averaging across worms (for EPG recordings) or wells (for wMicroTracker experiments). Sigmoidal concentration-response curves were fit to the data according to a Hill equation:

$$H_i = R_\infty + (R_0 - R_\infty)\cdot\left(\frac{b^r}{b^r + \frac{f}{1-f}x_i^r}\right)$$

where H_i is the theoretical response at drug concentration x_i, R_0 and R_∞ are, respectively, the responses when $x_i = 0$ and $x_i = \infty$, r is the Hill coefficient, and b is the concentration of drug that blocked fraction f of the maximal block ($b = IC_{50}$ for $f = 0.5$; $b = IC_{95}$ for $f = 0.95$). Except where noted (see Fig. 8), R_∞ was constrained to equal 0 (complete block of the response at high drug concentration), leaving 3 fitted parameters (R_0, b, r), which were chosen to minimize $\sum_i \frac{(H_i - m_i)^2}{2\sigma_i^2}$. This weighted least squares criterion yields the maximum likelihood value of IC_{50}, assuming that the measurement errors are drawn from independent Gaussian distributions. To test for significant differences between IC_{50} values between pairs of concentration-response curves we performed an additional, weighted least squares fit in which IC_{50} was constrained to be the same for both concentration-response curves, leaving 5 free parameters, which is one fewer than the 6 free parameters (3 for each fit) needed to fit the two concentration-response curves separately. We then calculated the log likelihood ratio as:

$$\ln\Lambda = \sum_i \frac{(H_i' - m_i)^2}{2\sigma_i^2} + \sum_j \frac{\left(H_j' - m_j\right)^2}{2\sigma_j^2} - \sum_i \frac{(H_i - m_i)^2}{2\sigma_i^2} - \sum_j \frac{(H_j - m_j)^2}{2\sigma_j^2}$$

where the subscripts i and j denote the points on the two concentration-response curves H_i and H_j and H_i' and H_j' denote Hill curves constrained to have the same IC_{50} for both concentration-response curves. The test statistic $-2\ \ln\Lambda$ is distributed approximately as χ^2 with 1 degree of freedom (Wolfram Math World, http://mathworld.wolfram.com/LikelihoodRatio.html, 2017), from which we determined two-tailed p-values.

For clarity of graphical display, concentration-response curves in Figs. 2, 4 and 8 were re-scaled after fitting by dividing each fitted curve and the corresponding data points by R_0, such that all of the fitted curves

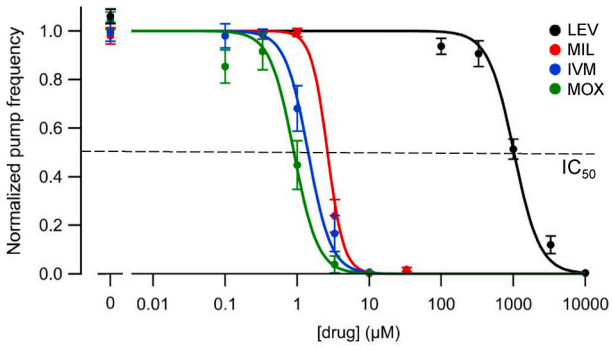

Fig. 4. Effects of MLs and LEV on pump frequency in the 8-channel platform. The panel shows plots (mean ± S.E.M.) of normalized mean pump frequencies during a 5 min epoch from $t = 55$–60 min plotted against drug concentration for the three MLs and LEV (color legend in the key). Pump frequencies were normalized to each worm's baseline pump frequency before averaging across worms. Hill curves were fit to the normalized data using a maximum likelihood criterion with three free parameters (see Methods); the dashed horizontal line at 0.5 intercepts the IC_{50} value for each drug. IC_{50} values and statistical comparisons are in Table 1. Hill slope coefficients: LEV, 2.4; MIL, 2.6; IVM, 1.4; MOX, 0.90. (For interpretation of the references to color in this figure legend, the reader is referred to the Web version of this article.)

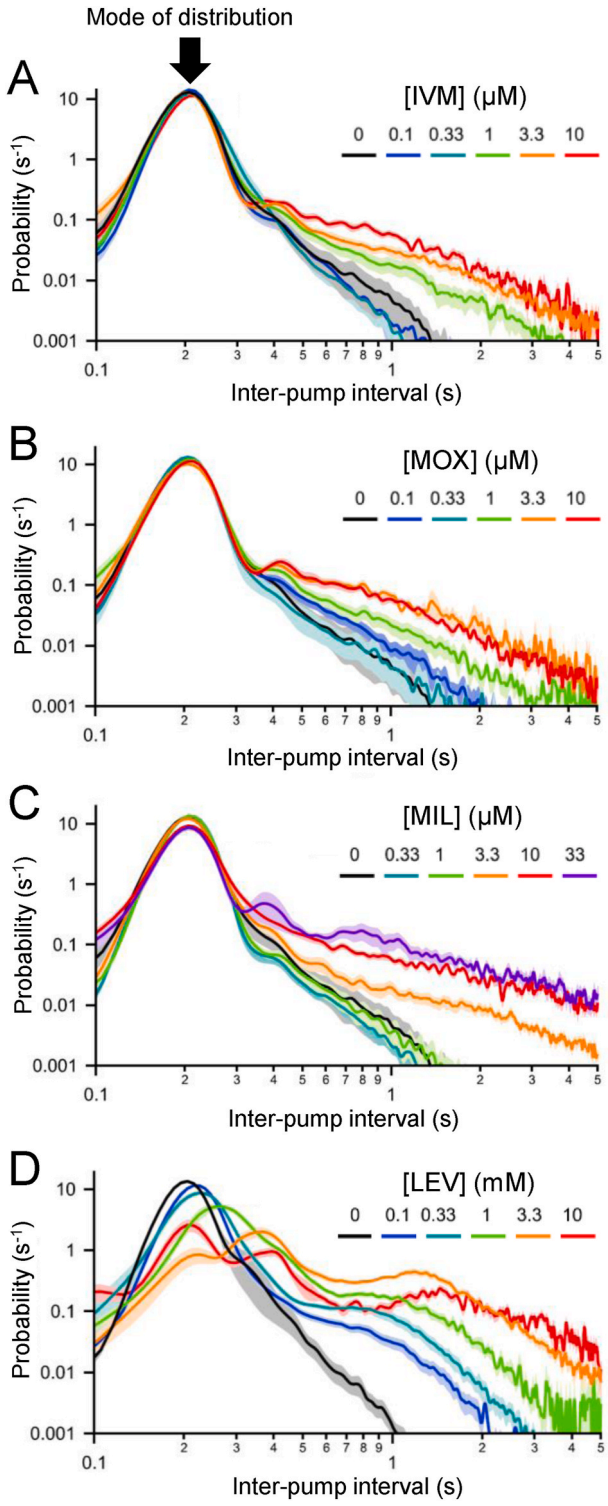

Fig. 5. Effects of MLs and LEV on the temporal pattern of pumping in the 8-channel platform. Inter-pump intervals (IPIs) were measured as the time between successive E spikes. A - D, IPI values during the epoch $t = 0$–60 min were plotted as probability density functions for three MLs and LEV (same data set as Fig. 3). Keys show color coding of drug concentrations. The mode (most probable value of IPI) is indicated by an arrow in A. In IVM, MOX and MIL (A–C), the mode was maintained at all concentrations tested while the probability of longer IPIs increased with drug concentration. Similarly, LEV (D) caused a concentration-dependent increase in the probability of longer IPIs but, unlike the MLs, additionally caused a rightward shift of the mode to longer IPIs. (For interpretation of the references to color in this figure legend, the reader is referred to the Web version of this article.)

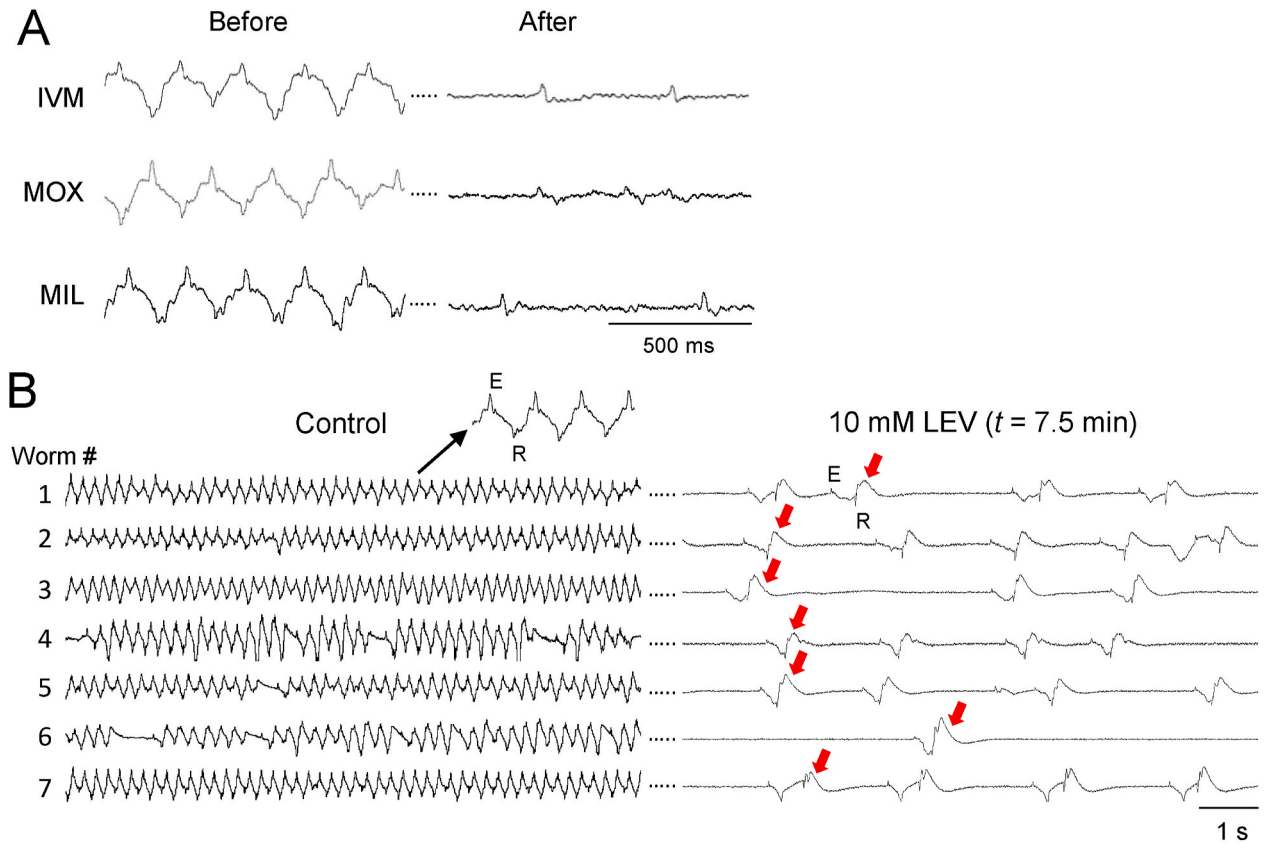

Fig. 6. Effects of MLs and LEV on EPG waveforms in the 8-channel platform. For each drug, worms were analyzed in 3 chips, with $n = 19$ to 22 worms per drug. We analyzed EPG waveforms of worms that ceased pumping after the perfusate switch; in LEV, the worms were in the sustained phase of inhibition following the switch (see Fig. 3G). A. Representative EPG waveforms in three MLs during the baseline period ("Before") and in the presence of the indicated ML, as pumping neared its end in individual worms ("After"; in 10 μM IVM, 1 μM MOX and 1 μM MIL). For each drug, Before and After traces are shown for the same worm. In all three MLs, EPG waveforms become smaller in amplitude and briefer. B. Representative changes in EPG waveforms in LEV. The traces are from seven worms in one chip, during the baseline period (left) and 7.5 min after switching to 10 mM LEV (right). E and R spikes persisted but a conspicuous "hump" appeared after R spikes (red arrows). (For interpretation of the references to color in this figure legend, the reader is referred to the Web version of this article.)

crossed the *x*-axis at y = 1. The reported IC_{50} and IC_{95} values, Hill coefficients, and *p*-values were calculated before rescaling. To reduce the effects of variability between worms, concentration-response data obtained using the 8-channel platform were normalized before averaging across worms, by dividing each worm's pump frequency after drug application by its baseline pump frequency (Weeks et al., 2018a, 2018b).

3. Results

3.1. Microfluidic chip systems allow recoding of anthelmintic drug effects on pharyngeal pumping

In the present study we recorded EPGs using the ScreenChip and 8-channel platform to study anthelmintic drug effects on pharyngeal pumping in *C. elegans*. For all experiments, Day-1 adult worms were incubated continuously with 10 mM 5HT ("M9-5HT") to drive robust and sustained pharyngeal pumping (Raizen and Avery, 1994) in the absence of drug treatment. In both chips, M9-5HT elicited steady pumping at a frequency of ~4–5 Hz, with occasional gaps between pumping bouts (see below), providing a baseline against which inhibitory drug effects could be observed. Four different anthelmintic drugs were tested: three MLs (IVM, MOX and MIL) plus LEV; the former are GluCl agonists whereas LEV is an agonist of L-type nAChRs (Dent et al., 1997, 2000; Martin et al., 2012; Holden-Dye and Walker, 2014). Drugs were tested at five or more concentrations, from which concentration-response curves for inhibition of pharyngeal pumping were calculated to assess drug potencies. Experimental protocols differed based on which EPG chip was used (Fig. 1A and B).

3.1.1. EPG recordings using the ScreenChip

Drug incubations were initiated 30 min before worms were loaded into the ScreenChip, after which 30-s EPG recordings were made for 30 min (Fig. 1Aiii). Total drug exposure time thus ranged between 30 and 60 min. Fig. 2A shows representative EPG recordings from two individual worms in ScreenChips, treated with a low (0.01 μM) or higher (0.3 μM) concentration of IVM. The higher concentration caused total cessation of pumping. Fig. 2B shows that all four drugs caused concentration-dependent inhibition of pharyngeal pumping. Concentration-response curves were generated to derive IC_{50} values, allowing drug potencies to be ranked. The IC_{50} values and their statistical comparisons are shown in Table 1 (Supplemental Table 1 contains IC_{95} values). In the ScreenChip, MOX and IVM were the most potent drugs and their IC_{50} values did not differ significantly. MIL was next in potency, followed by LEV, which had an IC_{50} value approximately three orders of magnitude higher than those of the MLs.

3.1.2. EPG recordings using the 8-channel platform

Fig. 3A, B and C shows EPG recordings from three 8-channel chips with different drug treatments. In each case, pumping was strong and regular during the baseline period. Switching the M9-5HT perfusate to the same solution (Fig. 3A) caused no noticeable effect on pumping, with the exception that Worm 4 showed a brief gap in activity. In contrast, switching perfusate to 10 μM MOX or 3.3 mM LEV (Fig. 3B and C) caused

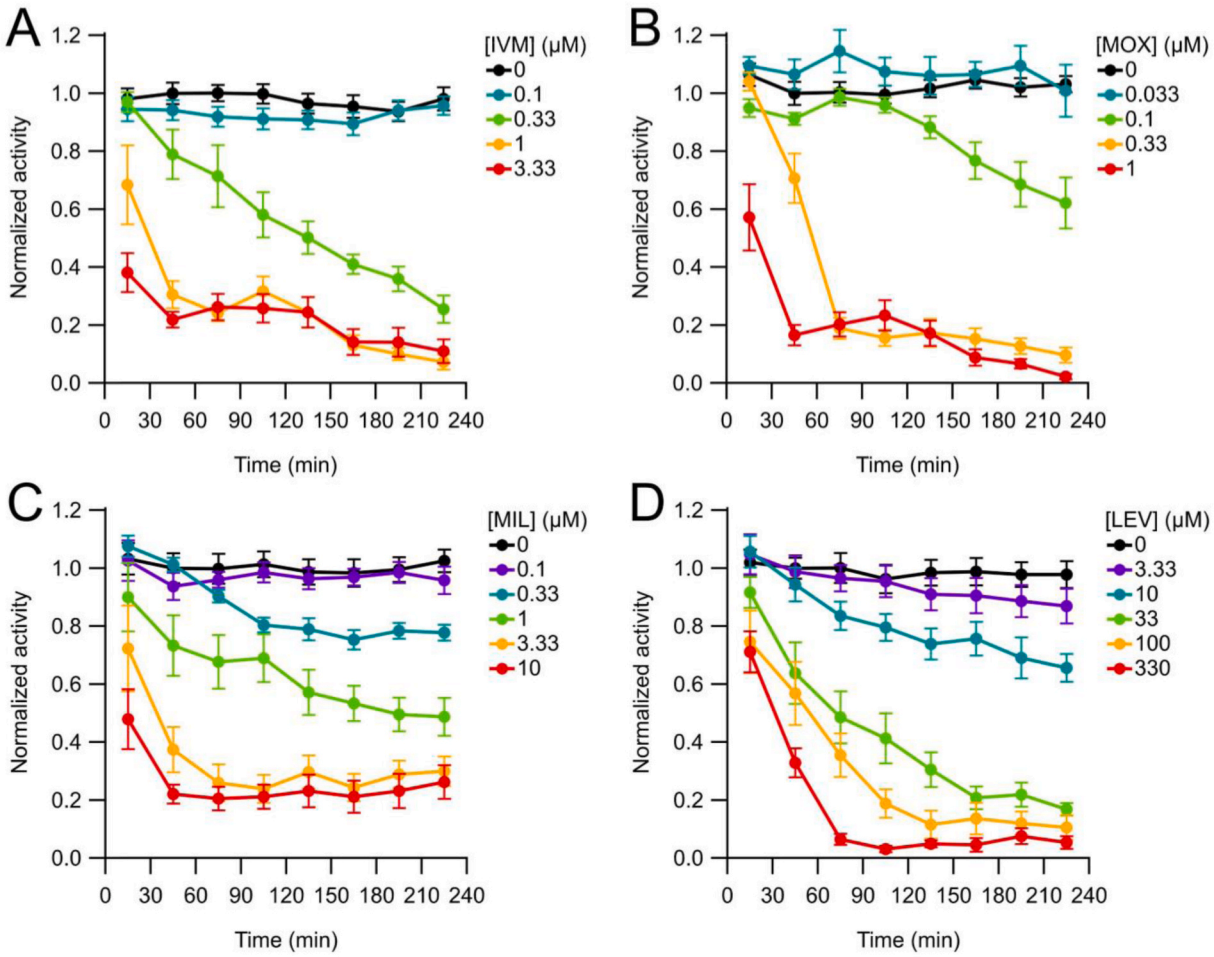

Fig. 7. Time course of ML and LEV effects on motility in the wMicroTracker. A – D are plots of normalized activity (mean ± S.E.M.; see Methods) over time in different concentrations of the drugs indicated. Activity was recorded continuously for 4 h and binned into 30 min epochs for analysis. Points in the plots are centered in the middle of each time bin. The MLs (A–C) and LEV (D) all caused a concentration-dependent decrease in motility over time.

marked reductions in pumping, although the time course differed for the two drugs.

Fig. 3D, E, F and G show plots of pump frequency versus time for the four drugs tested. In each case, inhibition of pumping was both concentration- and time-dependent. For IVM and MOX, reliable inhibitory effects were first observed at a concentration of 1 μM, with complete inhibition of pumping at 10 μM. In MIL, inhibition was first apparent at 3.3 μM and complete inhibition of pumping occurred at 10 μM. Unlike MLs, LEV had a biphasic effect, with a rapid initial reduction of pump frequency followed by a partial recovery (Weeks et al., 2018b). Only the highest concentration of LEV tested (10 mM) completely inhibited pumping by the end of the 60 min exposure.

Concentration-response curves were generated (Fig. 4) using mean pump frequency values during the final 5 min of the recording period (t = 55–60 min; from Fig. 3D, E, F and G). The order of potency of the four drugs in the 8-channel platform was the same as for ScreenChip experiments, but IC_{50} values were 2- to 20-fold higher (Table 1). The reduced effectiveness of drugs in the 8-channel platform compared to the ScreenChip may result from the different microchannel architecture and the experimental protocols used (see Discussion). Finally, the IC_{50} values of MOX and IVM differed significantly in the 8-channel experiments, whereas they did not in ScreenChip experiments (Table 1). Supplemental Table 1 contains IC_{95} values.

EPG recordings from the 8-channel platform revealed additional phenotypes caused by anthelmintic drugs. The pumping rhythm (i.e., steady vs. irregular) was revealed by plotting probability distributions of inter-pump intervals (IPIs), defined as the time from the beginning of one pump to the beginning of the next (E-spike to E-spike interval). Fig. 5 shows IPI plots for the four tested drugs. The three MLs (Fig. 5A–C) all showed similar distributions, in which the mode remained stable at an IPI of ~200–250 ms (corresponding to ~ 4–5 Hz), over the full range of drug concentrations, while the probability of IPIs > 500 ms increased with increasing drug concentration. This pattern corresponds to highly regular pumping interrupted by occasional pauses that become longer and more frequent as the drug concentration increases. In contrast, LEV (Fig. 5D) caused both the mode and the right shoulder of the IPI distribution to shift toward longer intervals as drug concentration increased. This represents a concentration-dependent slowing of the overall pumping rhythm as well as an increase in the probability, and duration, of pauses. The IVM and LEV distributions in Fig. 5 replicate results reported by Weeks et al. (2018b) but, importantly, the present results demonstrate that the probability-distribution phenotype caused by IVM is shared by other MLs and may thus be a drug-class defining feature. Furthermore, the ML phenotype differs markedly from that of LEV. Whether the LEV phenotype is shared by other drugs in its class remains to be determined.

The 8-channel EPG recordings revealed another phenotype that differed between the MLs and LEV. Lockery et al. (2012) reported that EPG waveforms become progressively briefer (i.e., E-spike to R-spike interval decreases) and smaller in amplitude in IVM. Fig. 6A shows representative EPG recordings from three different worms before and after treatment with IVM, MOX or MIL. The IVM result replicates the

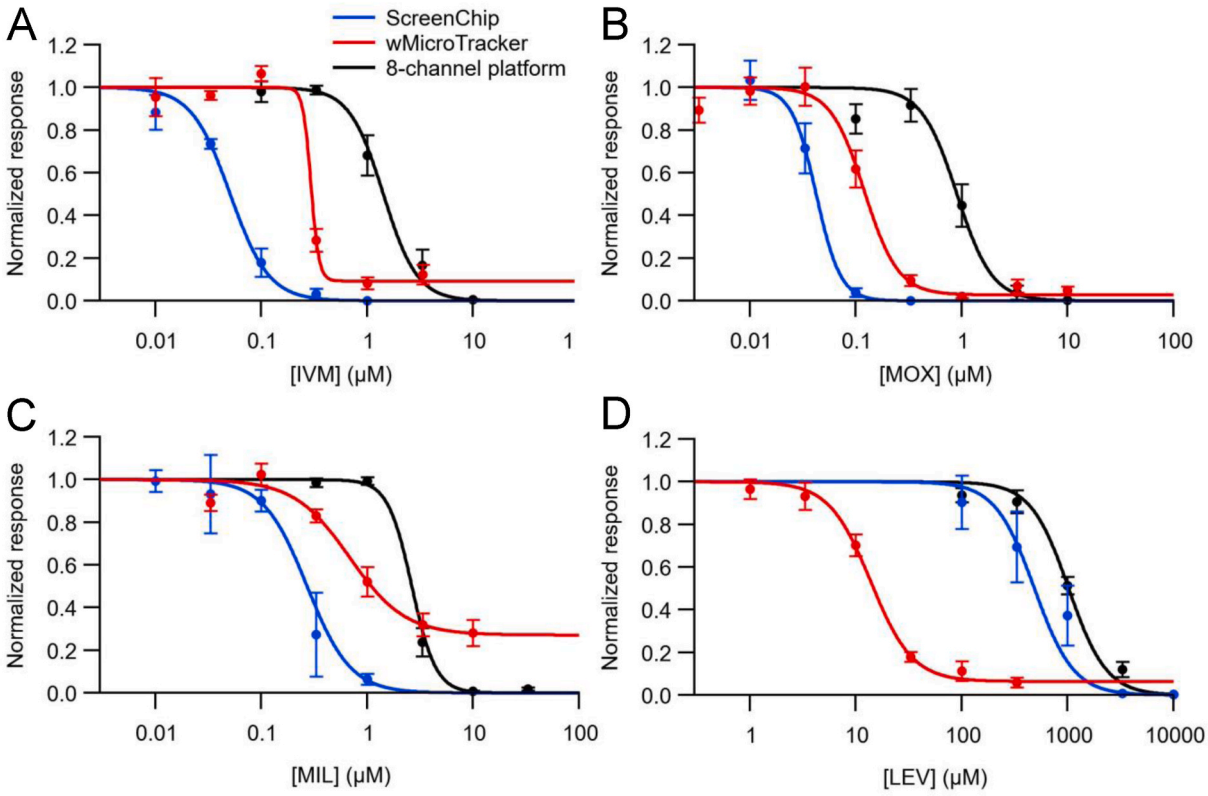

Fig. 8. Comparison of concentration-response curves from different assays. Each panel shows concentration-response curves for one drug, using the three assays indicated. Key in A applies to all panels. ScreenChip and 8-channel curves are repeated from Figs. 2 and 4, respectively, while wMicroTracker curves were plotted from the final time bin (t = 210–240 min) shown in Fig. 7. IC_{50} values and statistics for wMicroTracker data are shown in Table 1. Hill slope coefficients for wMicroTracker data were: IVM, 2.7; MOX, 2.6; MIL, 3.8; LEV, 2.4.

Table 1
Overview of IC50 values obtained with the three assay systems.

	IC_{50} (μM)		
	ScreenChip (pump frequency) t = 30–60 min	8-channel chip (pump frequency) t = 55–60 min	wMicroTracker (motility) t = 210–240 min
MOX	0.042	0.90	0.12
IVM	0.051	1.42	0.29
MIL	0.27	2.64	0.68
LEV	485	982	13.8

IC_{50} values were defined as the drug concentration that produced 50% of the maximal inhibition, which was incomplete for wMicroTracker experiments (see Fig. 8). All pairwise comparisons in the same column were significant at $p < 10^{-8}$ except: MOX and IVM did not differ significantly in ScreenChip recordings ($p = 0.25$) and were modestly different in 8-channel recordings ($p = 0.025$); IVM and MIL were significantly different in 8-channel recordings ($p = 0.0026$). All pairwise comparisons of IC_{50} values in the same row were significant at $p < 10^{-8}$ except for two of the ScreenChip vs wMicroTracker comparisons: MIL, $p = 0.0014$; MOX, $p = 0.0049$; and the ScreenChip vs 8-channel comparison: LEV, $p = 0.13$. All comparisons were made by a 2-tailed likelihood ratio test (Weeks et al., 2018a), not corrected for multiple comparisons.

previous finding of Lockery et al. (2012) but additionally shows that this waveform phenotype is shared by all three MLs tested. In contrast, LEV caused a very different waveform phenotype, in which a pronounced "hump" began to follow each R spike (Fig. 6B). This waveform shape was occasionally observed in ML-treated worms, but it was a brief and transient phenotype (data not shown). During the sustained phase of inhibition in LEV, as pumping slowed and eventually stopped in higher drug concentrations, the hump became less pronounced and waveform amplitudes became smaller (data not shown). The post-R-spike hump does not appear to correspond to any waveform features described by others (Franks et al., 2006) and determining its functional correlates would require additional experiments. As found for the IPI probability distributions, EPG waveform phenotypes in the presence of a drug may likewise represent a drug-class defining feature, but additional members of the drug classes should be tested.

3.2. *Evaluation of drug effects on worm motility using the WMicroTracker*

The ion channel targets of ML and LEV drug classes are present on body wall muscles and these drugs have well-characterized effects on the motility of *C. elegans* and other nematode species (Kass et al., 1980; Dent et al., 2000; Martin et al., 2005; Ardelli et al., 2009; Holden-Dye and Walker, 2014). To assay the effects of these drugs on the motility of Day-1 adult *C. elegans*, we used the wMicroTracker device (InVivo Biosystems). This LED-based assay system records drug effects on nematode motility over time, in a 96-well microtiter plate format (Liu et al., 2019; Risi et al., 2019). All four drugs tested showed concentration- and time-dependent effects on *C. elegans* motility over a 4-h recording period (Fig. 7); worms incubated without drug retained normal activity whereas increasing drug concentrations caused motility to decline more rapidly and to a greater extent. For MOX, inhibitory effects were first observed at a concentration of 0.1 μM, with nearly complete inhibition induced at the two highest concentrations (0.33 and 1 μM). The other MLs, IVM and MIL, were less potent in this motility assay. Inhibition of motility in IVM and MIL was first observed at 0.33 μM; IVM produced nearly complete paralysis at the two highest concentrations (1 and 3.33 μM) whereas MIL caused a maximum reduction of only 80% even at the two highest concentrations applied (3.33 and 10 μM). By comparison, LEV reduced *C. elegans* motility at a minimum concentration of 10 μM, with nearly complete paralysis at 100 and 330 μM.

Table 2
Comparison of properties of the three different assay systems.

	ScreenChip System	8-channel Platform	wMicroTracker
Device	Microfluidic chip with PDMS matrix; one EPG recording module	Microfluidic chip with PDMS matrix; eight recording modules	LED-based assay device for microtiter plates (24-, 96-, or 384-well format)
Phenotypic read-out	Pharyngeal pumping (EPG recordings)	Pharyngeal pumping (EPG recordings)	Whole nematode motility recordings
Experimental format	Short-term EPG recordings of individual worms in quick succession, in series Drug incubation occurs in a pre-recording step	Long-term EPG recordings from up to eight worms in parallel Continuous perfusion of test solution; switching perfusate allows baseline and drug recordings on the same worms	Long-term motility recordings of worms suspended in liquid Image-free recording, no microscope or image analysis software required
Type of data/ analyses	Generates concentration-response curves of pump frequency May permit IPI and waveform shape analysis	Generates concentration-response curves of pump frequency, and time-course of drug effects Recordings allow analysis of other parameters (e.g., IPIs, waveform shapes) Within-subjects statistical design	Generates concentration-response curves and time-course of drug effects Offers within-plate replicates
Limitations	Not designed for long-term recordings No perfusion of test solutions possible	Less sensitive (higher IC50s) than ScreenChip, perhaps due to more PDMS drug absorption	No visual evaluation of drug effects possible during recordings unless plate is removed from instrument
Suitability for different *C. elegans* life stages	Can be used with different life stages (different cartridge sizes available)	Routinely used for adult *C. elegans;* chips can be adapted for smaller worms (unpublished data)	Successfully used for adults (this study) and larval stages of *C. elegans*: e.g., L4 (Risi et al., 2019)
Suitability for other species	*Haemonchus contortus* (unpublished data)	*Ancylostoma ceylanicum* § and L4 stages and *A. caninum* L4 stage, *Ascaris suum* L3 stage (Weeks et al., 2016). Also *H. contortus* L4 stage, *Panagrellus redivivus* adult and *Pristionchus pacificus* adult (https://invivobiosystems.com/view-from-the-bench/microfluidic-epg-recordings-from-diverse-nematode-species/)	*Brugia pahangi* (L3, adults), *Cooperia oncophora* (L3), *H. contortus* (L3), *Ostertagia ostertagi* (L3) *Teladorsagiacircumcincta*(L3), and trematode *Schistosoma mansoni* (schistosomulas) (Liu et al., 2019; Gunderson et al., 2020)
Ease of use	Requires standard worm-handling skills but no electrophysiology skills	Requires electrophysiology skills	Requires standard worm-handling skills
Availability	Commercially available	Not commercially available	Commercially available

Concentration-response plots of drug effects on worm motility are shown in Fig. 8, for comparison with the EPG platforms (see below). Motility values from the final data interval during the experiment (t = 210–240 min) were plotted; this interval was selected because the motility values had reached or nearly reached asymptotic levels (Fig. 7). IC_{50} values and their statistical comparisons are shown in Table 1. MLs were more effective at inhibiting motility than LEV, with the most potent drug being MOX, followed by IVM and MIL. LEV had an IC_{50} value approximately 20- to 100-fold higher than that of the MLs (Table 1). Supplemental Table 1 contains IC_{95} values.

3.3. Comparison of concentration-response curves of the three platforms

For ease of comparison, Fig. 8 combines concentration-response curves for all four drugs, each tested in three assay systems. Each panel combines the curves obtained from ScreenChip, 8-channel platform and wMicroTracker experiments for that drug. When comparing the curves, note that the plotted data were collected at different times after the onset of drug exposure: ScreenChip, t = 30–60 min; 8-channel platform, t = 55–60 min; and wMicroTracker, t = 210–240 min. The data collection times were thus most similar for the ScreenChip and 8-channel platform. As seen in Fig. 8A, B, C and Table 1, for the three MLs tested, the lowest IC_{50} value was obtained with the ScreenChip, followed by the wMicroTracker, followed by the 8-channel platform. If expressed as assay sensitivity to the ML drugs tested, the order is ScreenChip > wMicroTracker > 8-channel platform (most to least sensitive). Below, we discuss possible reasons for the higher IC_{50} values measured in the 8-channel platform versus the ScreenChip.

In contrast, for LEV, Fig. 8D and Table 1, the lowest IC_{50} value was obtained with the wMicroTracker, followed by the ScreenChip, followed by the 8-channel platform. To investigate the potential effect of extended exposure duration on the IC_{50} value obtained for LEV in the wMicroTracker, we plotted a separate concentration-response curve using data from the 30–60 min data interval shown in Fig. 7. The derived IC_{50} value for this curve was 54.0 μM (data not shown), which is still an order of magnitude smaller than the IC_{50} values for LEV obtained in the ScreenChip or 8-channel platform (Table 1). Thus, the order of assay sensitivity to LEV is wMicroTracker > ScreenChip > 8-channel platform (most to least sensitive).

4. Discussion

4.1. Use of multiple assay systems to characterize anthelmintic effects

A majority of anthelmintic drugs exert their effects by impairing neuromuscular function in nematodes, and the neuromuscular system remains an important focus for developing next-generation drugs (Martin and Robertson, 2010; Wolstenholme, 2011). To understand the mode of action and target specificity of drug candidates, assays that can capture subtle and tissue-specific phenotypes are of great value. Moreover, assay combinations that read out multiple phenotypes can help reveal unique compound characteristics and prioritize promising drug candidates.

In the present study we selected four well characterized anthelmintic drugs — three MLs (IVM, MOX, MIL), and LEV — as references to evaluate their effects on the pharyngeal and body-wall neuromuscular system of *C. elegans*. To this end, we used three different phenotypic read-outs that focus either on the pharynx (ScreenChip, 8-Channel platform) or the body wall musculature (wMicroTracker) of the nematode. Table 2 summarizes the strengths and limitations of these assays, as highlighted below.

The two pharyngeal pumping assays both rely on electrical recording of pharyngeal activity but are optimized for different purposes. The ScreenChip is a commercial product and designed to be user-friendly for investigators with no prior electrophysiology experience. It allows EPGs to be recorded from many worms in quick succession. In the protocol we

applied here, 30-s EPG recordings were made from 45 to 60 individual worms per experimental group during the time interval $t = 30–60$ min after drug onset, in three replicates. Data from this 30-min interval were combined, providing no time-course information; time-course data in this study were obtained using the 8-channel platform. It is possible to obtain time-course data from ScreenChip recordings by increasing the sample size and combining EPG recordings into time bins based on when they were made with respect to drug onset. In theory, longer-duration EPG recordings of individual worms in the ScreenChip could provide time-course data, but the chip is not designed to hold a worm in position for extended periods. The ScreenChip is also not designed for perfusing test solutions while recording.

The 8-channel platform is optimized to obtain long EPG recordings from eight worms simultaneously, with continuous drug perfusion and the ability to rapidly switch perfusate solution (Lockery et al., 2012; Weeks et al., 2018b). For example, in this study, we recorded EPGs under baseline conditions for 15 min, switched perfusate, and recorded for 60 min more. Features of this platform include the ability to obtain time-course data and observe slowly-developing drug effects (Fig. 3). Long-duration recordings also aid in interpreting changes in pump patterning or waveform shape (Figs. 5 and 6), which typically evolve over time. Finally, because each worm serves as its own control, the 8-channel platform permits within-subjects statistical analyses, which increases statistical power. Unlike the ScreenChip, the 8-channel platform is not commercially available. It has been used at the University of Oregon and at InVivo Biosystems and is currently best suited for users with electrophysiology experience.

To examine drug effects on body wall muscles, we used the wMicroTracker to measure worm motility. Paralysis, i.e., the loss of motility, is a classic phenotype used to detect anthelmintic bioactivity. Advantages of the wMicroTracker are the higher-throughput format of 96-well microtiter plates (or 24- or 384-well plates) and the ability to set up within-plate replicates. A unique feature of the wMicroTracker is that it does not image worms but rather counts interruptions of a miniature LED beam as worms move in the liquid medium. While eliminating the need for a microscope and image analysis software, it is sometimes useful to observe worms during drug treatments; this would require removing the plate from the wMicroTracker and using a microscope. Gunderson et al. (2020) have compared the relative advantages of measuring parasite motility using the WormAssay and Worminator imaging systems, versus the wMicroTracker.

4.2. Findings from EPG recordings

The inhibitory effect of ML, especially of IVM, on the pharynx of *C. elegans* and other nematodes is well described (Avery and Horvitz, 1990; Geary et al., 1993; Holden-Dye and Walker, 2006). Acting as agonists of GluCls, MLs interfere with normal neuromuscular function in nematodes. AVR-15, for example, one of the ML-susceptible GluCl subunits in *C. elegans*, is expressed on pharyngeal muscles; M3 pharyngeal motor neurons activate these GluCls, to synaptically inhibit the muscles and terminate each pharyngeal pump (Dent et al., 1997; Avery and You, 2012). Electrophysiological studies have measured pronounced effects of IVM on the dissected *C. elegans* pharynx, with EC_{50} values for GluCl activation of 2–3 nM (Pemberton et al., 2001; Holden-Dye and Walker, 2006). Because the nematode cuticle is a barrier to small molecules (Ruiz-Lancheros et al., 2011), higher drug concentrations are expected to be effective for intact worms compared to isolated pharynges. Indeed, Weeks et al. (2018b) reported that a *bus-8* mutant (Partridge et al., 2008), which has an enhanced permeability of the cuticle, showed significantly greater sensitivity to IVM compared to the N2 reference strain. Another factor that may have affected drug potency in our experiments is potential absorption of drugs into the PDMS layer of the microfluidic chips (see below). In our hands, when applied to intact worms in a background of 5HT-stimulated pumping (which could potentially oppose pump inhibition by applied drugs), IVM and MOX showed comparable activities in a low nanomolar range in the ScreenChip (IC_{50} of 0.051 μM and 0.042 μM, respectively; Table 1), which are somewhat higher than those reported for worms tested on drug-treated agar plates or liquid culture (Ardelli et al., 2009; Bygarski et al., 2014; Castro et al., 2020).

Interestingly, IVM and MOX belong to different sub-classes of ML, the avermectins and milbemycins, respectively, which derive from different *Streptomyces* species. Both sub-classes differ in distinct structural features (Shoop et al., 1995) and some studies also provide evidence for sub-class specific differences in their effects on nematodes (Lespine et al., 2007; Ardelli et al., 2009; Lloberas et al., 2013; Bygarski et al., 2014). Ardelli et al. (2009) performed a comprehensive comparison of IVM and MOX using the *C. elegans* reference strain N2, and different GluCl knock-out mutants. In their experiments, IVM was 8-fold more potent in inhibiting pharyngeal pumping then MOX when N2 worms were exposed to the drugs on NGM agar plates (Ardelli et al., 2009). However, a direct comparison of anthelmintic concentration-response data from different studies are complicated by different read-outs, incubation times, drug application mode (e.g., liquid medium vs. solid medium), and other factors. As mentioned above, in our ScreenChip experiments, IVM and MOX were equally potent, while the IC_{50} value of MIL (milbemycin sub-class) was almost 6-fold higher than that of IVM and MOX (Table 1). These results suggesting that derivative-specific differences within a sub-class might play a more important role in potency than sub-class per se, at least for *C. elegans*. In comparison, our 8-channel EPG data showed a similar order of potency but with uniformly higher IC_{50} values (discussed below).

In contrast to MLs, the effects of LEV on the nematode pharynx have been less studied. LEV is an agonist of a sub-class of nAChRs, the L-type (L-) nAChRs. L-nAChRs are present on body wall muscles, where they mediate excitatory synaptic transmission, but are absent from the pharynx and direct application of LEV on the dissected pharynx does not affect pumping (Fleming et al., 1997; Culetto et al., 2004; Towers et al., 2005; Holden-Dye and Walker, 2014). Instead, the hallmark of LEV's anthelmintic activity is a pronounced hyper-contracting paralysis of the whole worm (Holden-Dye and Walker, 2014), which is induced in *C. elegans* at a low micromolar concentrations of LEV (Qian et al., 2008; Sloan et al., 2015; Ding et al., 2017) (see below). Nevertheless, despite the absence of L-nAChRs in the *C. elegans* pharynx, previous studies using the 8-channel platform reported inhibitory effects of LEV on pharyngeal pumping at concentrations of 1 mM and higher (Lockery et al., 2012; Weeks et al., 2018b). Here, we reproduced these former results with both chip platforms. In the ScreenChip and 8-channel platform, LEV was the least effective drug in inhibiting pharyngeal pumping, with IC_{50} values of 485 μM and 982 μM, respectively (Table 1). Because L-nAChRs are reportedly missing from the pharynx, the effect of LEV on pharyngeal pumping is likely mediated indirectly. A recent study showed that optogenetic silencing of *C. elegans* body wall muscles can inhibit pharyngeal pumping (Takahashi and Takagi, 2017) but the mechanism of this indirect effect remains to be established. Given the high micromolar to millimolar LEV concentrations used in this study, receptors other than L-nAChRs could potentially have been affected; to our knowledge, activation of other classes of *C. elegans* AChRs by LEV have not been reported, but it remains a possibility.

The MLs and LEV differed in the time course of their effects. Inhibition of pharyngeal pumping by MLs began within the first 5 min of drug exposure and, for higher concentrations, terminated pumping completely by $t = 15–30$ min (Fig. 3D, E, F). Pump frequency decreased monotonically towards steady-state during the 60-min recording. In contrast, LEV had a more rapid onset of inhibition, followed by a partial recovery that sometimes reached steady-state by the end of the recording (Weeks et al., 2018b). A further difference between the drug classes was revealed by probability distributions of IPI (Fig. 5); with increasing concentrations of MLs, the modal frequency of pumping remained stable while gaps in the pumping rhythm became longer and more frequent. This pattern differed from LEV, which caused both the

modal pump frequency and the duration of gaps to increase. Pump frequency is the most common readout used in *C. elegans* studies, but time course data and IPI probability distributions obtained from long EPG recordings in the 8-channel platform provide additional phenotypes that, in our study, distinguished the MLs and LEV. Furthermore, MLs in both the avermectin and milbemycin sub-classes exhibited similar time-course and IPI distributions, consistent with a common mode of action on the *C. elegans* pharynx.

While the rankings of drug potency were the same for ScreenChip and the 8-channel platform, the IC_{50} values showed that drugs were 2- to 20-fold less potent in the latter platform. Both chips consist of a PDMS layer with microchannels, bonded to a glass substrate. It is well documented that PDMS absorbs small molecules, which cross the walls of the PDMS channels and diffuse into the material. The chemical properties of molecules affect absorption, with low molecular mass and high hydrophobicity being the most favorable properties (Gomez-Sjoberg et al., 2010; Auner et al., 2019). The MLs tested in this study, MOX, IVM and MIL, have molecular masses of 640, 875 and 529 g/mol, and XLogP-AA values of 4.3, 4.1 and 3.1, respectively (https://pubchem.ncbi.nlm.nih.gov/). These values are 204 g/mol and 1.8 for LEV. Higher XLogP-AA values indicate higher hydrophobicity. In other experiments, HPLC analysis showed that ML concentrations decrease as drugs are perfused through the 8-channel platform (Weeks, J.C., K.J. Robinson, A. Moghaddan, W.M. Roberts, unpublished data) but the relative importance of molecular weight vs. hydrophobicity for absorption has not been fully explored. A key difference between the ScreenChip and 8-channel platform is in the surface area of PDMS that the solution contacts while traversing the chip. The 8-channel chip has an extensive network of channels that distribute worms into recording modules, through which perfusate flows during an experiment, while the ScreenChip has a small reservoir followed by one relatively short channel and minimal movement of solution through the chip during an experiment (Fig. 1A and B). Thus, the opportunity for drug to be absorbed out of solution into PDMS was much greater for the 8-channel chip. Furthermore, in ScreenChip experiments, worms were pretreated with drugs for 30 min outside the chip before being loaded in the same drug solution. The only opportunity for drug absorption was when worms were in the ScreenChip.

Although other factors are possible, the increased likelihood of drug absorption into PDMS in the 8-channel platform compared to the ScreenChip may explain the higher IC_{50} values derived from 8-channel experiments. Interestingly, the IC_{50} values for LEV in the ScreenChip and 8-channel platform were the most similar among all the drugs tested on these platforms. Based on XLogP-AA, LEV is the least likely to enter PDMS, so drug absorption may have been less than for MLs. It is possible to reduce or eliminate the issue of PDMS absorption by pre-treating microchannels with particular chemical agents, or fabricating chips out of plastic or glass (Gomez-Sjoberg et al., 2010; Ren et al., 2011; Hirama et al. 2018; Gökaltun et al., 2019), which we did not explore in the present experiments. Short of that, our findings indicate that the ScreenChip is a better choice than the 8-channel platform for sensitive determinations of IC_{50} values based on EPG recordings.

4.3. Findings from motility assays

In addition to the pharynx, we evaluated the effects of all four anthelmintic drugs on the body wall musculature of adult *C. elegans* using the wMicroTracker. MLs, especially IVM, are well characterized for their inhibitory effect on *C. elegans* motility (Dent et al., 2000; Ardelli et al., 2009; Holden-Dye and Walker, 2014). Depending on their experimental protocols, former studies found IVM concentrations in a nanomolar to low micromolar range to be sufficient to inhibit *C. elegans* motility (Ardelli et al., 2009; Glendinning et al., 2011; Kearn et al., 2014; Ferreira et al., 2015; Weaver et al., 2017; Castro et al., 2020). For example, Glendinning et al. (2011) reported a complete paralysis of adult *C. elegans* at a concentration of 1 μM IVM. Risi et al. (2019) tested the effect of IVM on *C. elegans* L4 larvae using the wMicroTracker and observed an IC_{50} value of 0.19 μM. In our wMicroTracker experiments, we observed pronounced concentration- and time-dependent effects of MLs on *C. elegans* motility, with IC_{50} values of 0.12 μM for MOX and 0.29 μM for IVM.

Comparison of the time course of the inhibition of worm motility (wMicroTracker; Fig. 7), with the time course of inhibition of pumping (8-channel platform; Fig. 3), indicates that the latter occurred more rapidly. Furthermore, the IC_{50} values from the wMicroTracker were ~2.5–5.7 times higher than those measured in the ScreenChip (the more sensitive of the two EPG platforms; Table 1). ML-sensitive GluCls are expressed in both pharynx and body wall muscles, but the pharynx might be exposed to drugs more rapidly by ingestion of the drug solution. Ingestion of IVM is reported to be unnecessary for the induction of paralysis (Smith and Campbell, 1996; O'Lone and Campbell, 2001) but it could nevertheless have contributed to the speed and potency of ML effects on the pharynx in our experiments. In summary, MOX, IVM and MIL act more rapidly and at lower concentrations on the pharynx than on body wall muscles, as assayed behaviorally by pharyngeal pumping and motility; this finding comports with the tissue location of these drugs' targets.

As with the MLs, LEV is well known to induce paralysis of the body wall muscle in *C. elegans* and other nematodes (Holden-Dye and Walker, 2014). Using the wMicroTracker, we detected a continuous, concentration- and time-dependent decrease of *C. elegans* motility over the time-course of the experiment (Fig. 7D), which differed from the biphasic effect on pharyngeal pumping observed with the 8-channel platform (Fig. 3 G). The calculated IC_{50} value of 13.8 μM (Table 1) for LEV-induced paralysis compared favorably with concentration response data of former studies (Qian et al., 2008; Sloan et al., 2015; Ding et al., 2017; Blanco et al., 2018; Risi et al., 2019). For example, Qian et al. (2008) reported an IC_{50} value for LEV of 9 μM in their motility assays, while a PDMS-microfluidic chip approach reported a lower IC_{50} value of 2.2 μM (Ding et al., 2017). In addition, Risi et al. (2019), using the wMicroTracker, reported an IC_{50} value of 6.4 μM which is close to the result presented here. Direct comparison of both studies is difficult because, among other differences, Risi et al. (2019) tested LEV on *C. elegans* L4 larvae instead of adult worms.

In contrast to MLs, LEV appeared to be > 30 times more potent as an inhibitor of worm motility than as an inhibitor of pharyngeal pumping (Table 1). These findings are in accordance with the location of L-nAChRs in the body wall muscle and their absence in the pharynx of *C. elegans*. As discussed above (see section 4.2), the observed LEV effect on the pharynx is likely indirect and may result from the paralysis of the body wall muscle.

4.4. Conclusions

The aim of the present study was to compare two EPG recording platforms and the wMicroTracker to identify respective strengths and limitations of these assays for anthelmintic research. Table 2 summarizes these findings and includes additional comparisons such as ease-of-use and species compatibility, to help guide the application of these platforms.

We also evaluated potential advantages resulting from combined analysis of EPG and motility recordings. The ScreenChip proved sufficient to rank potencies of reference drugs on *C. elegans* pharyngeal pumping, while the 8-channel platform provided additional data including the time-course of drug effects and how drugs affected EPG temporal patterning and waveform shape. A marked difference in drug potencies between the two EPG platforms, especially for MLs, identified the ScreenChip as the more sensitive of the two assays. The wMicroTracker device allowed the generation of time-course data and IC_{50} values for all four drugs on *C. elegans* motility, which were in accordance with former studies.

Our combined analysis of EPG and whole worm motility recordings

revealed the characteristic effects of these well-studied anthelmintic drugs in accord with the location of their known molecular targets. This includes the pronounced effects of MLs on the nematode pharynx that, in our hands, acted faster and in lower concentrations compared to whole worm paralysis. For LEV, as expected, drug effects were observed on the body wall musculature at significantly lower concentrations before the pharynx was affected. Both drug classes showed distinct features such as time-courses of drug effects, modulation of EPG patterning and changes in EPG waveform. These may represent drug-class defining phenotypes, a hypothesis that can be explored further by testing additional drugs in the same, and other, classes. With respect to the ML class of anthelmintics, our results indicated that derivative-specific differences within a sub-class (avermectins or milbemycins) might be more relevant for potency than belonging to a certain sub-class. To address ML sub-class specific differences in a broader experimental context, the use of different *C. elegans* genetic backgrounds could help to address how target specificity, distribution, metabolism, and detoxification/excretion might influence ML potencies.

In summary, electrophysiological and motility assays of anthelmintic effects performed alone, or especially in combination, provide valuable insights into drug effects that can contribute to developing critically-needed anthelmintic therapies to advance animal, plant and human health. Additional studies, including testing a broader set of reference drugs from different anthelmintic drug classes, will be useful for further evaluating the value of this combined read-out approach.

Declaration of competing interest

Iring Heisler is an employee of Elanco Animal Health and Daniel Kulke, and Steffen R. Hahnel were employees of Elanco Animal Health at the time the work was undertaken. Elanco Animal Health develops and sells veterinary pharmaceuticals including dewormers. Janis C. Weeks and William M. Roberts hold equity in InVivo Biosystems Inc., a company that develops and sells laboratory devices such as microfluidic EPG chip platforms and the wMicroTracker reported here. Except for the authors, Elanco Animal Health and InVivo Biosystems Inc. were not involved in the preparation of the manuscript. The decision to publish the manuscript was jointly taken.

Acknowledgements

The authors thank Carolin Gojny, Sven Zymny and Kristin J. Robinson for excellent technical assistance. We further thank the Bayer Life Sciences Collaboration (LSC) for funding SRH.

Appendix A. Supplementary data

Supplementary data to this article can be found online at https://doi.org/10.1016/j.ijpddr.2021.05.005.

References

Ardelli, B.F., Stitt, L.E., Tompkins, J.B., Prichard, R.K., 2009. A comparison of the effects of ivermectin and moxidectin on the nematode Caenorhabditis elegans. Vet. Parasitol. 165, 96–108.

Auner, A.W., Tasneem, K.M., Markov, D.A., McCawley, L.J., Hutson, M.S., 2019. Chemical-PDMS binding kinetics and implications for bioavailability in microfluidic devices. Lab Chip 19, 864–874.

Avery, L., Horvitz, H.R., 1990. Effects of starvation and neuroactive drugs on feeding in Caenorhabditis elegans. J. Exp. Zool. 253, 263–270.

Avery, L., You, Y.J., 2012. C. elegans feeding. WormBook 1–23.

Blanchard, A., Guegnard, F., Charvet, C., Crisford, A., Courtot, E., Sauvé, C., Harmache, A., Duguet, T., O'Connor, V., Castagnone-Sereno, P., Reaves, B., Wolstenholme, A.J., Beech, R.N., Holden-Dye, L., Neveu, C., 2018. Deciphering the molecular determinants of cholinergic anthelmintic sensitivity in nematodes: when novel functional validation approaches highlight major differences between the model Caenorhabditis elegans and parasitic species. PLoS Pathog. 14, e1006996.

Blanco, M.G., Vela Gurovic, M.S., Silbestri, G.F., Garelli, A., Giunti, S., Rayes, D., De Rosa, M.J., 2018. Diisopropylphenyl-imidazole (DII): a new compound that exerts anthelmintic activity through novel molecular mechanisms. PLoS Neglected Trop. Dis. 12, e0007021.

Brownlee, D.J., Holden-Dye, L., Walker, R.J., 1997. Actions of the anthelmintic ivermectin on the pharyngeal muscle of the parasitic nematode, Ascaris suum. Parasitology 115 (Pt 5), 553–561.

Burns, A.R., Luciani, G.M., Musso, G., Bagg, R., Yeo, M., Zhang, Y., Rajendran, L., Glavin, J., Hunter, R., Redman, E., Stasiuk, S., Schertzberg, M., Angus McQuibban, G., Caffrey, C.R., Cutler, S.R., Tyers, M., Giaever, G., Nislow, C., Fraser, A.G., MacRae, C.A., Gilleard, J., Roy, P.J., 2015. Caenorhabditis elegans is a useful model for anthelmintic discovery. Nat. Commun. 6, 7485.

Bygarski, E.E., Prichard, R.K., Ardelli, B.F., 2014. Resistance to the macrocyclic lactone moxidectin is mediated in part by membrane transporter P-glycoproteins: implications for control of drug resistant parasitic nematodes. Int. J. Parasitol. Drugs Drug Resist. 4, 143–151.

Calahorro, F., Keefe, F., Dillon, J., Holden-Dye, L., O'Connor, V., 2019. Neuroligin tuning of pharyngeal pumping reveals extrapharyngeal modulation of feeding in Caenorhabditis elegans. J. Exp. Biol. 222 (Pt 3), jeb189423.

Castro, M.J., Turani, O., Faraoni, M.B., Gerbino, D., Bouzat, C., 2020. A new antagonist of Caenorhabditis elegans glutamate-activated chloride channels with anthelmintic activity. Front. Neurosci. 14, 879.

Colquhoun, L., Holden-Dye, L., Walker, R.J., 1991. The pharmacology of cholinoceptors on the somatic muscle cells of the parasitic nematode Ascaris suum. J. Exp. Biol. 158, 509–530.

Cook, A., Franks, C.J., Holden-Dye, L., 2006. Electrophysiological recordings from the pharynx. WormBook 1–7.

Culetto, E., Baylis, H.A., Richmond, J.E., Jones, A.K., Fleming, J.T., Squire, M.D., Lewis, J.A., Sattelle, D.B., 2004. The Caenorhabditis elegans unc-63 gene encodes a levamisole-sensitive nicotinic acetylcholine receptor alpha subunit. J. Biol. Chem. 279, 42476–42483.

Cully, D.F., Vassilatis, D.K., Liu, K.K., Paress, P.S., Van der Ploeg, L.H., Schaeffer, J.M., Arena, J.P., 1994. Cloning of an avermectin-sensitive glutamate-gated chloride channel from Caenorhabditis elegans. Nature 371, 707–711.

Demeler, J., von Samson-Himmelstjerna, G., Sangster, N.C., 2014. Measuring the effect of avermectins and milbemycins on somatic muscle contraction of adult Haemonchus contortus and on motility of Ostertagia circumcincta in vitro. Parasitology 141, 948–956.

Dent, J.A., Davis, M.W., Avery, L., 1997. avr-15 encodes a chloride channel subunit that mediates inhibitory glutamatergic neurotransmission and ivermectin sensitivity in Caenorhabditis elegans. EMBO J. 16, 5867–5879.

Dent, J.A., Smith, M.M., Vassilatis, D.K., Avery, L., 2000. The genetics of ivermectin resistance in Caenorhabditis elegans. Proc. Natl. Acad. Sci. U. S. A. 97, 2674–2679.

Diawara, A., Halpenny, C.M., Churcher, T.S., Mwandawiro, C., Kihara, J., Kaplan, R.M., Streit, T.G., Idaghdour, Y., Scott, M.E., Basáñez, M.G., Prichard, R.K., 2013. Association between response to albendazole treatment and β-tubulin genotype frequencies in soil-transmitted helminths. PLoS Neglected Trop. Dis. 7, e2247.

Ding, X., Njus, Z., Kong, T., Su, W., Ho, C.M., Pandey, S., 2017. Effective drug combination for Caenorhabditis elegans nematodes discovered by output-driven feedback system control technique. Sci. Adv. 3, eaao1254.

Ferreira, S.R., Mendes, T.A., Bueno, L.L., de Araújo, J.V., Bartholomeu, D.C., Fujiwara, R. T., 2015. A new methodology for evaluation of nematode viability. BioMed Res. Int. 2015, 879263.

Fleming, J.T., Squire, M.D., Barnes, T.M., Tornoe, C., Matsuda, K., Ahnn, J., Fire, A., Sulston, J.E., Barnard, E.A., Sattelle, D.B., Lewis, J.A., 1997. Caenorhabditis elegans levamisole resistance genes lev-1, unc-29, and unc-38 encode functional nicotinic acetylcholine receptor subunits. J. Neurosci. 17, 5843–5857.

Franks, C.J., Holden-Dye, L., Bull, K., Luedtke, S., Walker, R.J., 2006. Anatomy, physiology and pharmacology of Caenorhabditis elegans pharynx: a model to define gene function in a simple neural system. Invertebr. Neurosci. 6, 105–122.

Geary, T.G., Sims, S.M., Thomas, E.M., Vanover, L., Davis, J.P., Winterrowd, C.A., Klein, R.D., Ho, N.F., Thompson, D.P., 1993. Haemonchus contortus: ivermectin-induced paralysis of the pharynx. Exp. Parasitol. 77, 88–96.

Gill, J.H., Redwin, J.M., van Wyk, J.A., Lacey, E., 1991. Detection of resistance to ivermectin in Haemonchus contortus. Int. J. Parasitol. 21, 771–776.

Glendinning, S.K., Buckingham, S.D., Sattelle, D.B., Wonnacott, S., Wolstenholme, A.J., 2011. Glutamate-gated chloride channels of Haemonchus contortus restore drug sensitivity to ivermectin resistant Caenorhabditis elegans. PloS One 6, e22390.

Gomez-Sjoberg, R., Leyrat, A.A., Houseman, B.T., Shokat, K., Quake, S.R., 2010. Biocompatibility and reduced drug absorption of sol-gel-treated poly(dimethyl siloxane) for microfluidic cell culture applications. Anal. Chem. 82, 8954–8960.

Gökaltun, A., Kang, Y., Yarmush, M.L., Usta, O.B., Asatekin, A., 2019. Simple surface modification of poly(dimethylsiloxane) via surface segregating smart polymers for biomicrofluidics. Sci. Rep. 9 (1), 7377.

Gunderson, E., Bulman, C., Luo, M., Sakanari, J., 2020. In vitro screening methods for parasites: the wMicroTracker & the WormAssay. MicroPubl. Biol. (Epub 2020/07/25) https://doi.org/10.17912/micropub.biology.000279, 10.17912.

Hirama H, Satoh T, Sugiura S, Shin K, Onuki-Nagasaki R, Kanamori T, Inoue T. Glass-based organ-on-a-chip device for restricting small molecular absorption. J. Biosci. Bioeng. 127(5):641-646.

Holden-Dye, L., Walker, R.J., 2006. Actions of glutamate and ivermectin on the pharyngeal muscle of Ascaridia galli: a comparative study with Caenorhabditis elegans. Int. J. Parasitol. 36, 395–402.

Holden-Dye, L., Walker, R.J., 2014. Anthelmintic Drugs and Nematicides: Studies in Caenorhabditis elegans. WormBook., pp. 1–29

Hotez, P.J., Alvarado, M., Basanez, M.G., Bolliger, I., Bourne, R., Boussinesq, M., Brooker, S.J., Brown, A.S., Buckle, G., Budke, C.M., Carabin, H., Coffeng, L.E., Fevre, E.M., Furst, T., Halasa, Y.A., Jasrasaria, R., Johns, N.E., Keiser, J., King, C.H.,

Lozano, R., Murdoch, M.E., O'Hanlon, S., Pion, S.D., Pullan, R.L., Ramaiah, K.D., Roberts, T., Shepard, D.S., Smith, J.L., Stolk, W.A., Undurraga, E.A., Utzinger, J., Wang, M., Murray, C.J., Naghavi, M., 2014. The global burden of disease study 2010: interpretation and implications for the neglected tropical diseases. PLoS Neglected Trop. Dis. 8, e2865.

Hu, C., Dillon, J., Kearn, J., Murray, C., O'Connor, V., Holden-Dye, L., Morgan, H., 2013. NeuroChip: a microfluidic electrophysiological device for genetic and chemical biology screening of Caenorhabditis elegans adult and larvae. PloS One 8, e64297.

Hu, C., Kearn, J., Urwin, P., Lilley, C.V.O.C., Holden-Dye, L., Morgan, H., 2014. StyletChip: a microfluidic device for recording host invasion behaviour and feeding of plant parasitic nematodes. Lab Chip 14, 2447–2455.

Huang, C., Wagner-Valladolid, S., Stephens, A.D., Jung, R., Poudel, C., Sinnige, T., Lechler, M.C., Schlörit, N., Lu, M., Laine, R.F., Michel, C.H., Vendruscolo, M., Kaminski, C.F., Kaminski Schierle, G.S., David, D.C., 2019. Intrinsically aggregation-prone proteins form amyloid-like aggregates and contribute to tissue aging in Caenorhabditis elegans. eLife 8, e43059.

Kashyap, S.S., Verma, S., Voronin, D., Lustigman, S., Kulke, D., Robertson, A.P., Martin, R.J., 2019. Emodepside has sex-dependent immobilizing effects on adult Brugia malayi due to a differentially spliced binding pocket in the RCK1 region of the SLO-1 K channel. PLoS Pathog. 15, e1008041.

Kass, I.S., Wang, C.C., Walrond, J.P., Stretton, A.O., 1980. Avermectin B1a, a paralyzing anthelmintic that affects interneurons and inhibitory motoneurons in Ascaris. Proc. Natl. Acad. Sci. U. S. A. 77, 6211–6215.

Kearn, J., Ludlow, E., Dillon, J., O'Connor, V., Holden-Dye, L., 2014. Fluensulfone is a nematicide with a mode of action distinct from anticholinesterases and macrocyclic lactones. Pestic. Biochem. Physiol. 109, 44–57.

Kotze, A.C., Hunt, P.W., Skuce, P., von Samson-Himmelstjerna, G., Martin, R.J., Sager, H., Krucken, J., Hodgkinson, J., Lespine, A., Jex, A.R., Gilleard, J.S., Beech, R. N., Wolstenholme, A.J., Demeler, J., Robertson, A.P., Charvet, C.L., Neveu, C., Kaminsky, R., Rufener, L., Alberich, M., Menez, C., Prichard, R.K., 2014. Recent advances in candidate-gene and whole-genome approaches to the discovery of anthelmintic resistance markers and the description of drug/receptor interactions. Int. J. Parasitol. Drugs Drug Resist. 4, 164–184.

Krücken, J., Fraundorfer, K., Mugisha, J.C., Ramunke, S., Sifft, K.C., Geus, D., Habarugira, F., Ndoli, J., Sendegeya, A., Mukampunga, C., Bayingana, C., Aebischer, T., Demeler, J., Gahutu, J.B., Mockenhaupt, F.P., von Samson-Himmelstjerna, G., 2017. Reduced efficacy of albendazole against Ascaris lumbricoides in Rwandan schoolchildren. Int. J. Parasitol. Drugs Drug Resist. 7, 262–271.

Lai, Y., Xiang, M., Liu, S., Li, E., Che, Y., Liu, X., 2014. A novel high-throughput nematicidal assay using embryo cells and larvae of Caenorhabditis elegans. Exp. Parasitol. 139, 33–41.

Lespine, A., Martin, S., Dupuy, J., Roulet, A., Pineau, T., Orlowski, S., Alvinerie, M., 2007. Interaction of macrocyclic lactones with P-glycoprotein: structure-affinity relationship. Eur. J. Pharmaceut. Sci. 30, 84–94.

Liu, M., Landuyt, B., Klaassen, H., Geldhof, P., Luyten, W., 2019. Screening of a drug repurposing library with a nematode motility assay identifies promising anthelmintic hits against Cooperia oncophora and other ruminant parasites. Vet. Parasitol. 265, 15–18.

Lloberas, M., Alvarez, L., Entrocasso, C., Virkel, G., Ballent, M., Mate, L., Lanusse, C., Lifschitz, A., 2013. Comparative tissue pharmacokinetics and efficacy of moxidectin, abamectin and ivermectin in lambs infected with resistant nematodes: impact of drug treatments on parasite P-glycoprotein expression. Int. J. Parasitol. Drugs Drug Resist. 3, 20–27.

Lockery, S.R., Hulme, S.E., Roberts, W.M., Robinson, K.J., Laromaine, A., Lindsay, T.H., Whitesides, G.M., Weeks, J.C., 2012. A microfluidic device for whole-animal drug screening using electrophysiological measures in the nematode C. elegans. Lab Chip 12, 2211–2220.

Lustigman, S., Prichard, R.K., Gazzinelli, A., Grant, W.N., Boatin, B.A., McCarthy, J.S., Basanez, M.G., 2012. A research agenda for helminth diseases of humans: the problem of helminthiases. PLoS Neglected Trop. Dis. 6, e1582.

Martin, R.J., Robertson, A.P., 2000. Electrophysiological investigation of anthelmintic resistance. Parasitology 120 (Suppl. l), S87–S94.

Martin, R.J., Robertson, A.P., 2010. Control of nematode parasites with agents acting on neuro-musculature systems: lessons for neuropeptide ligand discovery. Adv. Exp. Med. Biol. 692, 138–154.

Martin, R.J., Robertson, A.P., Buxton, S.K., Beech, R.N., Charvet, C.L., Neveu, C., 2012. Levamisole receptors: a second awakening. Trends Parasitol. 28, 289–296.

Martin, R.J., Verma, S., Levandoski, M., Clark, C.L., Qian, H., Stewart, M., Robertson, A. P., 2005. Drug resistance and neurotransmitter receptors of nematodes: recent studies on the mode of action of levamisole. Parasitology 131 (Suppl. l), S71–S84.

Muthaiyan Shanmugam, M., Subhra Santra, T., 2016. Microfluidic Devices in Advanced Caenorhabditis elegans Research. Molecules, Basel, Switzerland, p. 21.

O'Lone, R.B., Campbell, W.C., 2001. Effect of refrigeration on the antinematodal efficacy of ivermectin. J. Parasitol. 87, 452–454.

Partridge, F.A., Brown, A.E., Buckingham, S.D., Willis, N.J., Wynne, G.M., Forman, R., Else, K.J., Morrison, A.A., Matthews, J.B., Russell, A.J., Lomas, D.A., Sattelle, D.B., 2018. An automated high-throughput system for phenotypic screening of chemical libraries on C. elegans and parasitic nematodes. Int. J. Parasitol. Drugs Drug Resist. 8, 8–21.

Partridge, F.A., Tearle, A.W., Gravato-Nobre, M.J., Schafer, W.R., Hodgkin, J., 2008. The C. elegans glycosyltransferase BUS-8 has two distinct and essential roles in epidermal morphogenesis. Dev. Biol. 317, 549–559.

Pemberton, D.J., Franks, C.J., Walker, R.J., Holden-Dye, L., 2001. Characterization of glutamate-gated chloride channels in the pharynx of wild-type and mutant Caenorhabditis elegans delineates the role of the subunit GluCl-alpha2 in the function of the native receptor. Mol. Pharmacol. 59, 1037–1043.

Qian, H., Robertson, A.P., Powell-Coffman, J.A., Martin, R.J., 2008. Levamisole resistance resolved at the single-channel level in Caenorhabditis elegans. Faseb. J. 22, 3247–3254.

Raizen, D.M., Avery, L., 1994. Electrical activity and behavior in the pharynx of Caenorhabditis elegans. Neuron 12, 483–495.

Ren, K., Dai, W., Zhou, J., Su, J., Wu, H., 2011. Whole-Teflon microfluidic chips. Proc. Natl. Acad. Sci. U. S. A. 108, 8162–8166.

Richmond, J.E., 2006. Electrophysiological recordings from the neuromuscular junction of C. elegans. WormBook 1–8.

Risi, G., Aguilera, E., Lados, E., Suarez, G., Carrera, I., Álvarez, G., Salinas, G., 2019. Caenorhabditis elegans infrared-based motility assay identified new hits for nematicide drug development. Vet. Sci. 6 (1), 29.

Ruiz-Lancheros, E., Viau, C., Walter, T.N., Francis, A., Geary, T.G., 2011. Activity of novel nicotinic anthelmintics in cut preparations of Caenorhabditis elegans. Int. J. Parasitol. 41, 455–461.

San-Miguel, A., Lu, H., 2013. Microfluidics as a tool for C. elegans research. WormBook 1–19.

Schwab, A.E., Boakye, D.A., Kyelem, D., Prichard, R.K., 2005. Detection of benzimidazole resistance-associated mutations in the filarial nematode Wuchereria bancrofti and evidence for selection by albendazole and ivermectin combination treatment. Am. J. Trop. Med. Hyg. 73, 234–238.

Shoop, W.L., Mrozik, H., Fisher, M.H., 1995. Structure and activity of avermectins and milbemycins in animal health. Vet. Parasitol. 59, 139–156.

Sloan, M.A., Reaves, B.J., Maclean, M.J., Storey, B.E., Wolstenholme, A.J., 2015. Expression of nicotinic acetylcholine receptor subunits from parasitic nematodes in Caenorhabditis elegans. Mol. Biochem. Parasitol. 204, 44–50.

Smith, H., Campbell, W.C., 1996. Effect of ivermectin on Caenorhabditis elegans larvae previously exposed to alcoholic immobilization. J. Parasitol. 82, 187–188.

Spensley, M., Del Borrello, S., Pajkic, D., Fraser, A.G., 2018. Acute effects of drugs on Caenorhabditis elegans movement reveal complex responses and plasticity. G3 (Bethesda) 8, 2941–2952.

Stasiuk, S.J., MacNevin, G., Workentine, M.L., Gray, D., Redman, E., Bartley, D., Morrison, A., Sharma, N., Colwell, D., Ro, D.K., Gilleard, J.S., 2019. Similarities and differences in the biotransformation and transcriptomic responses of Caenorhabditis elegans and Haemonchus contortus to five different benzimidazole drugs. Int. J. Parasitol. Drugs Drug Resist. 11, 13–29.

Stiernagle, T., 2006. Maintenance of C. elegans. WormBook 1–11.

Takahashi, M., Takagi, S., 2017. Optical silencing of body wall muscles induces pumping inhibition in Caenorhabditis elegans. PLoS Genet. 13, e1007134.

Towers, P.R., Edwards, B., Richmond, J.E., Sattelle, D.B., 2005. The Caenorhabditis elegans lev-8 gene encodes a novel type of nicotinic acetylcholine receptor alpha subunit. J. Neurochem. 93, 1–9.

Verma, S., Kulke, D., McCall, J.W., Martin, R.J., Robertson, A.P., 2020. Recording drug responses from adult Dirofilaria immitis pharyngeal and somatic muscle cells. Int. J. Parasitol. Drugs Drug Resist. 15, 1–8.

Weaver, K.J., May, C.J., Ellis, B.L., 2017. Using a health-rating system to evaluate the usefulness of Caenorhabditis elegans as a model for anthelmintic study. PloS One 12, e0179376.

Weeks, J.C., Roberts, W.M., Leasure, C., Suzuki, B.M., Robinson, K.J., Currey, H., Wangchuk, P., Eichenberger, R.M., Saxton, A.D., Bird, T.D., Kraemer, B.C., Loukas, A., Hawdon, J.M., Caffrey, C.R., Liachko, N.F., 2018a. Sertraline, paroxetine, and chlorpromazine are rapidly acting anthelmintic drugs capable of clinical repurposing. Sci. Rep. 8, 975.

Weeks, J.C., Roberts, W.M., Robinson, K.J., Keaney, M., Vermeire, J.J., Urban Jr., J.F., Lockery, S.R., Hawdon, J.M., 2016. Microfluidic platform for electrophysiological recordings from host-stage hookworm and Ascaris suum larvae: a new tool for anthelmintic research. Int. J. Parasitol. Drugs Drug Resist. 6, 314–328.

Weeks, J.C., Robinson, K.J., Lockery, S.R., Roberts, W.M., 2018b. Anthelmintic drug actions in resistant and susceptible C. elegans revealed by electrophysiological recordings in a multichannel microfluidic device. Int. J. Parasitol. Drugs Drug Resist. 8, 607–628.

Wolstenholme, A.J., 2011. Ion channels and receptor as targets for the control of parasitic nematodes. Int. J. Parasitol. Drugs Drug Resist. 1, 2–13.

Wolstenholme, A.J., Rogers, A.T., 2005. Glutamate-gated chloride channels and the mode of action of the avermectin/milbemycin anthelmintics. Parasitology 131 (Suppl. l), S85–S95.

Zamanian, M., Cook, D.E., Zdraljevic, S., Brady, S.C., Lee, D., Lee, J., Andersen, E.C., 2018. Discovery of genomic intervals that underlie nematode responses to benzimidazoles. PLoS Neglected Trop. Dis. 12, e0006368.

Zhu, B., Mak, J.C.H., Morris, A.P., Marson, A.G., Barclay, J.W., Sills, G.J., Morgan, A., 2020. Functional analysis of epilepsy-associated variants in STXBP1/Munc18-1 using humanized Caenorhabditis elegans. Epilepsia 61, 810–821.